4.5. In vivo biodistribution in normal mice

A saline solution (100 μL) of radiolabeled agents (0.2–0.4 μCi) containing ethanol (10 μL) was injected intravenously directly into the tail of ddY mice (5 weeks old, 25–30 g). The mice were sacrificed at various time points postinjection. The organs of interest were removed and weighed, and the radioactivity was measured with an automatic gamma counter (Aloka, ARC-380 or Perkin-Elmer 2470 wizard2).

Acknowledgments

The study was supported by a Grants-in Aid for Young Scientists (A) and Exploratory Research from the Ministry of Education, Culture, Sports, Science and Technology, the Program for Promotion of Fundamental Biomedical Innovation (NIBIO), and a Health Labor Sciences Research Grant.

Supplementary data

Supplementary data associated with this article can be found, in the online version, at doi:10.1016/j.bmc.2010.05.013.

References and notes

1. Klunk, W. E. *Neurobiol. Aging* **1998**, *19*, 145.
2. Selkoe, D. J. *Phys. Rev.* **2001**, *81*, 741.
3. Mathis, C. A.; Lopresti, B. J.; Klunk, W. E. *Nucl. Med. Biol.* **2007**, *34*, 809.
4. Mathis, C. A.; Wang, Y.; Klunk, W. E. *Curr. Pharm. Des.* **2004**, *10*, 1469.
5. Nordberg, A. *Lancet Neurol.* **2004**, *3*, 519.
6. Ono, M.; Wilson, A.; Norbrega, J.; Westaway, D.; Verhoeff, P.; Zhuang, Z. P.; Kung, M. P.; Kung, H. F. *Nucl. Med. Biol.* **2003**, *30*, 565.
7. Rowe, C. C.; Ackerman, U.; Browne, W.; Mulligan, R.; Pike, K. L.; O'Keefe, G.; Tochon-Danguy, H.; Chan, G.; Berlangieri, S. U.; Jones, G.; Dickinson-Rowe, K. L.; Kung, H. P.; Zhang, W.; Kung, M. P.; Skovronsky, D.; Dyrks, T.; Holl, G.; Krause, S.; Friebe, M.; Lehman, L.; Lindemann, S.; Dinkelborg, L. M.; Masters, C. L.; Villemagne, V. L. *Lancet Neurol.* **2008**, *7*, 129.
8. Choi, S. R.; Golding, G.; Zhuang, Z.; Zhang, W.; Lim, N.; Hefti, F.; Benedum, T. E.; Kilbourn, M. R.; Skovronsky, D.; Kung, H. F. *J. Nucl. Med.* **2009**, *50*, 1887.
9. Mathis, C. A.; Wang, Y.; Holt, D. P.; Huang, G. F.; Debnath, M. L.; Klunk, W. E. *J. Med. Chem.* **2003**, *46*, 2740.
10. Klunk, W. E.; Engler, H.; Nordberg, A.; Wang, Y.; Blomqvist, G.; Holt, D. P.; Bergstrom, M.; Savitcheva, I.; Huang, G. F.; Estrada, S.; Ausen, B.; Debnath, M. L.; Barletta, J.; Price, J. C.; Sandell, J.; Lopresti, B. J.; Wall, A.; Koivisto, P.; Antoni, G.; Mathis, C. A.; Langstrom, B., et al *Ann. Neurol.* **2004**, *55*, 306.
11. Johnson, A. E.; Jeppsson, F.; Sandell, J.; Wensbo, D.; Neelissen, J. A. M.; Juréus, A.; Ström, P.; Norman, H.; Farde, L.; Svensson, S. *J. Neurochem.* **2009**, *108*, 1177.
12. Nyberg, S.; Jönhagen, M. E.; Cselényi, Z.; Halldin, C.; Julin, P.; Olsson, H.; Freund-Levi, Y.; Andersson, J.; Varnäs, K.; Svensson, S.; Farde, L. *Eur. J. Nucl. Med. Mol. Imaging* **2009**, *11*, 1859.
13. Zhuang, Z. P.; Kung, M. P.; Hou, C.; Skovronsky, D.; Gur, T. L.; Trojanowski, J. Q.; Lee, V. M. Y.; Kung, H. F., et al *J. Med. Chem.* **2001**, *44*, 1905.
14. Zhuang, Z. P.; Kung, M. P.; Hou, C.; Plossel, K.; Skovronsky, D.; Gur, T. L.; Trojanowski, J. Q.; Lee, V. M. Y.; Kung, H. F. *Nucl. Med. Biol.* **2001**, *28*, 887.
15. Kung, M. P.; Hou, C.; Zhuang, Z. P.; Zhang, B.; Skovronsky, D.; Trojanowski, J. Q.; Lee, V. M.; Kung, H. F. *Brain Res.* **2002**, *956*, 202.
16. Newberg, A. B.; Wintering, N. A.; Plossl, K.; Hochold, J.; Stabin, M. G.; Watson, M.; Skovronsky, D.; Clark, C. M.; Kung, M. P.; Kung, H. F. *J. Nucl. Med.* **2006**, *47*, 748.
17. Ono, M.; Kung, M. P.; Hou, C.; Kung, H. F. *Nucl. Med. Biol.* **2002**, *29*, 633.
18. Ono, M.; Kawashima, H.; Nonaka, A.; Kawai, T.; Haratake, M.; Mori, H.; Kung, M. P.; Kung, H. F.; Saji, H.; Nakayama, M. *J. Med. Chem.* **2006**, *49*, 2725.
19. Chang, Y. S.; Jeong, J. M.; Lee, Y. S.; Kim, H. W.; Rai, B. G.; Kim, Y. J.; Lee, D. S.; Chung, J. K.; Lee, M. C. *Nucl. Med. Biol.* **2006**, *33*, 811.
20. Cai, L.; Cuevas, J.; Temme, S.; Herman, M. M.; Dagostin, C.; Widdowson, D. A.; Innis, R. B.; Pike, V. W. *J. Med. Chem.* **2008**, *51*, 148.
21. Cai, L.; Liow, J. S.; Zoghbi, S. S.; Cuevas, J.; Baetas, C.; Hong, J.; Shetty, H. U.; Seneca, N. M.; Brown, A. K.; Gladding, R.; Temme, S. S.; Herman, M. M.; Innis, R. B.; Pike, V. W. *J. Med. Chem.* **2007**, *50*, 4746.
22. Zeng, F.; Alagille, D.; Tamagnan, G. D.; Brian J. Ciliax, B. J.; Levey, A. I.; Goodman, M. M. *ACS Med. Chem. Lett.* ASAP. doi:10.1021/ml100005j.
23. Dishino, D. D.; Welch, M. J.; Kilbourn, M. R.; Raichle, M. E. *J. Nucl. Med.* **1983**, *24*, 1030.
24. Suzuki, N.; Yasaki, S.; Yasuhara, A.; Sakamoto, T. *Chem. Pharm. Bull.* **2003**, *10*, 1170.
25. Sano, H.; Noguchi, T.; Tanatani, A.; Hashimoto, Y.; Miyachi, H. *Bioorg. Med. Chem.* **2005**, *13*, 3079.
26. Arano, Y.; Wakisaka, K.; Ohmoto, Y.; Uezono, T.; Akizawa, H.; Nakayama, M.; Sakahara, H.; Tanaka, C.; Konishi, J.; Yokoyama, A. *Bioconjugate Chem.* **1996**, *7*, 628.
27. Kung, M. P.; Hou, C.; Zhuang, Z. P.; Skovronsky, D.; Kung, H. F. *Brain Res.* **2004**, *1025*, 98.
28. Chang, Y.; Prisoff, W. *Biochem. Pharmacol.* **1973**, *22*, 3099.

ACS Chemical Neuroscience pubs.acs.org/acschemicalneuroscience

Synthesis and Evaluation of Novel Chalcone Derivatives with ^{99m}Tc/Re Complexes as Potential Probes for Detection of β-Amyloid Plaques

Masahiro Ono,*[,†,‡] Ryoichi Ikeoka,[†] Hiroyuki Watanabe,[†] Hiroyuki Kimura,[‡] Takeshi Fuchigami,[†] Mamoru Haratake,[†] Hideo Saji,[‡] and Morio Nakayama*[,†]

[†]Graduate School of Biomedical Sciences, Nagasaki University, 1-14 Bunkyo-machi, Nagasaki 852-8521, Japan, and [‡]Graduate School of Pharmaceutical Sciences, Kyoto University, 46-29 Yoshida Shimoadachi-cho, Sakyo-ku, Kyoto 606-8501, Japan

Abstract

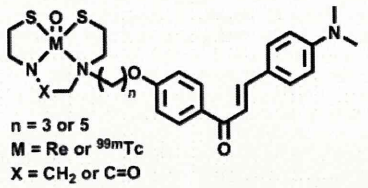

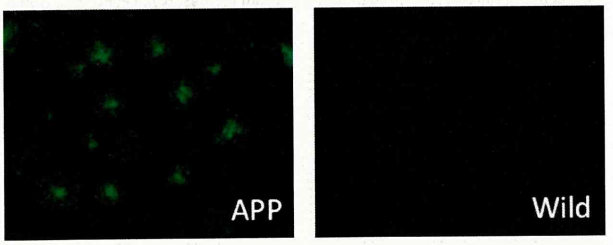

Four ^{99m}Tc-labeled chalcone derivatives and their corresponding rhenium analogues were tested as potential probes for imaging β-amyloid plaques. The chalcones showed higher affinity for Aβ(1−42) aggregates than did ^{99m}Tc complexes. In sections of brain tissue from an animal model of AD, the four Re chalcones intensely stained β-amyloid plaques. In biodistribution experiments using normal mice, ^{99m}Tc-BAT-chalcone ([^{99m}Tc]**17**) displayed high uptake in the brain (1.48% ID/g) at 2 min postinjection. The radioactivity washed out from the brain rapidly (0.17% ID/g at 60 min), a highly desirable feature for an imaging agent. [^{99m}Tc]**17** may be a potential probe for imaging β-amyloid plaques in Alzheimer's brains.

Keywords: Alzheimer's disease, β-amyloid plaque, ^{99m}Tc, single photon emission computed tomography (SPECT) imaging

Alzheimer's disease (AD), the most common senile dementia, is characterized by β-amyloid (Aβ) plaques, vascular amyloid, neurofibrillary tangles, and progressive neurodegeneration. The formation of plaques composed of β-amyloid peptides (Aβ) in the brain is considered the initial neurodegenerative event in AD (*1*). Thus, the detection of individual plaques *in vivo* by single photon emission tomography (SPECT) or positron emission tomography (PET) should improve diagnosis and also accelerate the discovery of effective therapeutic agents for AD (*2*−*4*).

Many radiolabeled probes for imaging β-amyloid based on Congo Red, thioflavin T, and DDNP have been reported. Among them, [^{11}C]PIB (*5*, *6*), [^{11}C]SB-13 (*7*, *8*), [^{18}F]BAY94-9172 (*9*, *10*), [^{11}C]BF-227 (*11*), [^{18}F]FDDNP (*12*, *13*), [^{123}I]IMPY (*14*−*16*), and [^{18}F]-AV-45 (*17*, *18*) have been tested clinically and demonstrated potential utility.

Recently, while searching for novel imaging probes, we found that ^{125}I-, ^{11}C-, and ^{18}F-labeled chalcone derivatives showed high affinity for Aβ aggregates and good uptake into and rapid clearance from the brain (*19*−*21*). In this study, we planned the development of novel chalcone derivatives labeled with technetium-99m (^{99m}Tc). ^{99m}Tc ($T_{1/2}$ = 6.01 h, 141 keV) has become the most commonly used radionuclide in diagnostic nuclear medicine for several reasons: it is readily produced by a ^{99}Mo/^{99m}Tc generator, the medium gamma-ray energy it emits is suitable for detection, and its physical half-life is compatible with the biological localization and residence time required for imaging. It is ready availability, essentially 24 h/day, and ease of use make it the radionuclide of choice. New ^{99m}Tc-labeled imaging agents will provide simple, convenient, and widespread SPECT-based imaging methods for detecting and eventually quantifying β-amyloid plaques in living brain tissue.

Kung et al. reported that a dopamine transporter imaging agent, [^{99m}Tc]TRODAT-1, is useful to detect the loss of dopamine neurons in the basal ganglia associated with Parkinson's disease. This is the first example of a ^{99m}Tc imaging agent that can penetrate the blood−brain barrier via a simple diffusion mechanism and localize at sites in the central nervous system. Based on this success, efforts were made to search for comparable ^{99m}Tc imaging

Received Date: April 27, 2010
Accepted Date: June 25, 2010
Published on Web Date: July 08, 2010

DOI: 10.1021/cn100042d | ACS Chem. Neurosci. (2010), 1, 598–607

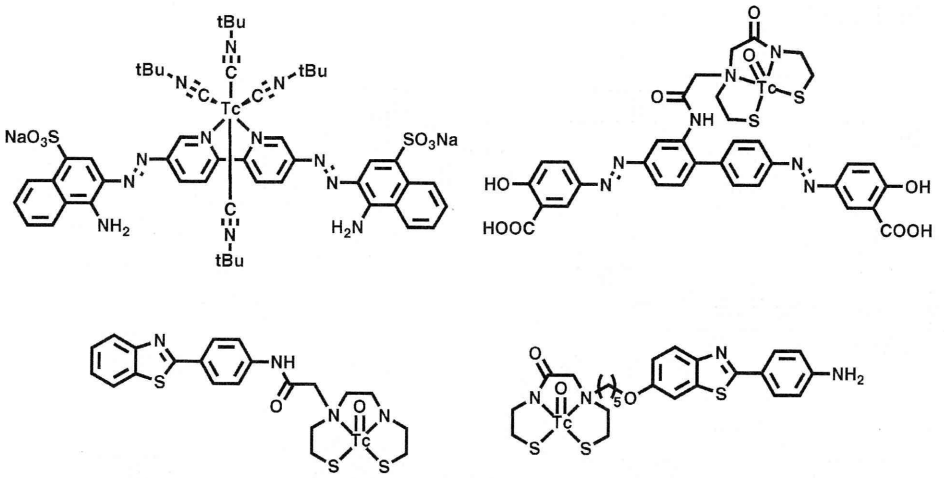

Figure 1. Chemical structure of ^{99m}Tc-labeled Aβ imaging probes reported previously.

Scheme 1. Synthesis of Chelation Ligands

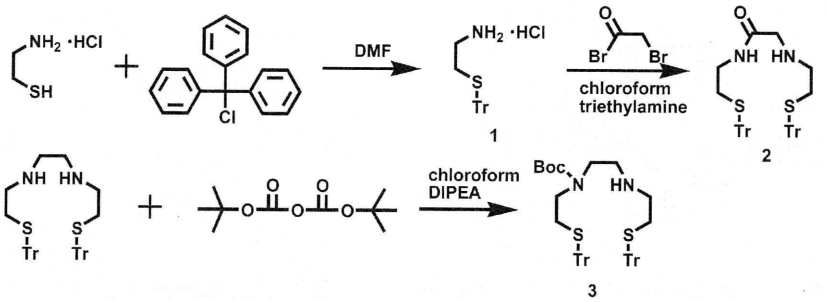

agents that target binding sites on β-amyloid plaques in the brain of AD patients. Several ^{99m}Tc-labeled imaging probes have been developed (Figure 1), but no clinical study of them has been reported (*22*−*25*).

In the present study, to develop more useful ^{99m}Tc-labeled probes for clinical diagnosis, we synthesized four chalcone derivatives with monoamine−monoamide dithiol (MAMA) and bis-amino-bis-thiol (BAT). MAMA and BAT were selected as chelation ligands taking into consideration the permeability of the blood−brain barrier, because they form an electrically neutral complex with ^{99m}Tc (*26*). We then evaluated their biological potential as probes by testing their affinity for Aβ aggregates and β-amyloid plaques in sections of brain tissue from Tg2576 mice and their uptake by and clearance from the brain in biodistribution experiments using normal mice. To our knowledge, this is the first time chalcones with ^{99m}Tc/Re complexes have been proposed as probes for the detection of β-amyloid plaques in the brain.

Results and Discussion

The synthesis of the ^{99m}Tc/Re chalcone derivatives is outlined in Schemes 1−3. The chelation ligands (MAMA and BAT) were synthesized according to methods reported previously with some slight modifications (Scheme 1) (*26*). The most useful method of preparing chalcones is the condensation of acetophenones with benzaldehydes(*19*). In this process, 4-hydroxybenzaldehyde was reacted with 4-dimethylaminobenzaldehyde in the presence of a basic catalyst (10% KOH) in ethanol at room temperature to form 4-dimethylamino-4′-hydroxy-chalcone (**4**) in a yield of 70%. The reaction of dibromo with **4** produced two chalcone derivatives (**5** and **6**) with alkyl groups (n = 3 or 5) of different lengths. Then, **5** (n = 5) or **6** (n = 3) was joined to **2** (Tr-MAMA) or **3** (Tr-Boc-BAT) to generate compounds **7** (n = 5) and **13** (n = 3) (Tr-MAMA-chalcones) or compounds **10** (n = 5) and **16** (n = 3) (Tr-Boc-BAT). Compounds **8**, **11**, **14**, and **17** (the precursors for ^{99m}Tc labeling) were obtained by deprotection of the thiol groups in **7**, **10**, **13**, and **16**, respectively. The Re complexes (**9**, **12**, **15**, and **18**) were prepared by the reaction of **7**, **11**, **13**, and **17** with $(PPh_3)_2ReOCl_3$. The corresponding ^{99m}Tc complexes, [^{99m}Tc]**8**, [^{99m}Tc]**11**, [^{99m}Tc]**14**, and [^{99m}Tc]**17**, were prepared by a ligand exchange reaction employing the precursor ^{99m}Tc-gluco-heptonate (GH). The resulting mixture was analyzed by reversed-phase HPLC, showing that a single radioactive complex formed with radiochemical purity higher than

DOI: 10.1021/cn100042d | ACS Chem. Neurosci. (2010), 1, 598–607

Scheme 2. Synthesis of Chalcone Derivatives

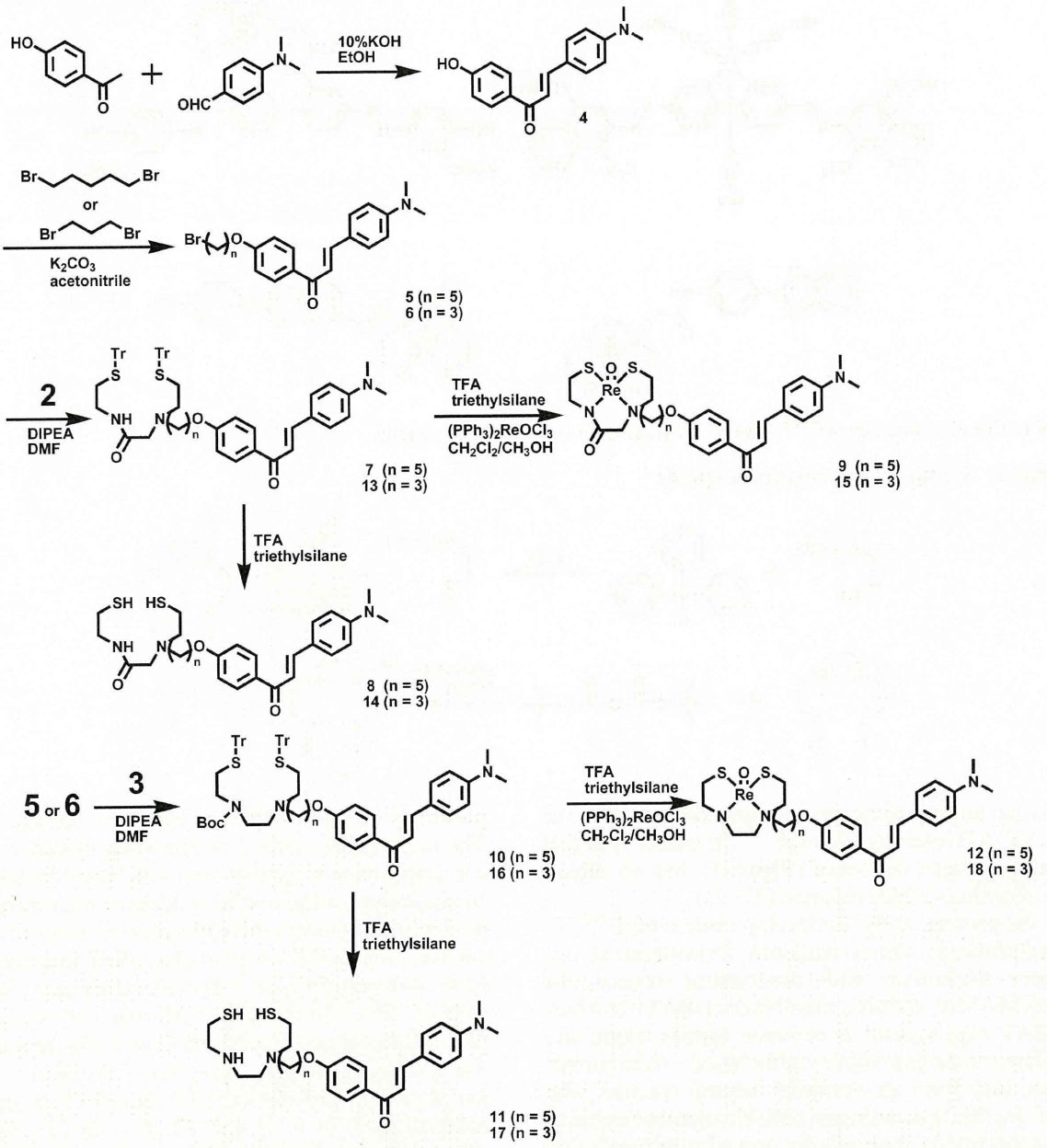

95% after purification by HPLC. The identity of the complex was established by comparative HPLC using the corresponding Re complexes as a reference (Table 1). The retention times for [^{99m}Tc]**8**, [^{99m}Tc]**11**, [^{99m}Tc]**14**, and [^{99m}Tc]**17** on HPLC (radioactivity) were 14.2, 20.3, 9.3, and 12.4 min, respectively. The retention times of the corresponding Re complexes on HPLC (UV detection) were 13.5, 18.4, 8.6, and 11.2 min, respectively.

In vitro binding experiments to evaluate the affinity of the ^{99m}Tc-labeled chalcones for Aβ aggregates were carried out in solutions (Figure 2). To make quantitative comparisons with ^{99m}Tc-BAT and ^{99m}Tc-MAMA, we showed the binding affinity as total Aβ(1−42) aggregate-bound radioactivity (%) at different concentrations of Aβ aggregates. In this assay, we also confirmed that the nonspecific Aβ(1−42) aggregate-bound radioactivity (%) was 1.9−3.2% in the four ^{99m}Tc-labeled chalcones, indicating that nearly all of the radioactivity occupied the specific binding site for Aβ aggregates. The percent radioactivity of the chalcones bound to aggregates increased dependent on the dose of Aβ(1−42). In terms of Aβ(1−42) aggregate-bound radioactivity, the derivatives ranked in the following

DOI: 10.1021/cn100042d | ACS Chem. Neurosci. (2010), 1, 598–607

Scheme 3. ^{99m}Tc Labeling of Chalcone Derivatives

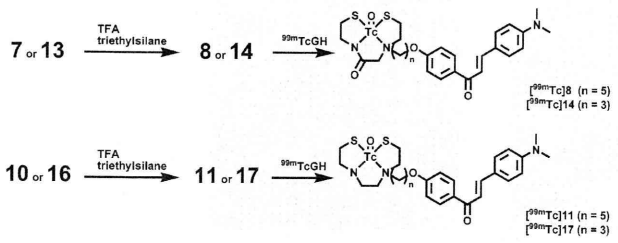

Table 1. HPLC Retention Times of ^{99m}Tc-Labeled Chalcones and Their Re Analogues and log *P* Values of ^{99m}Tc-Labeled Chalcones

^{99m}Tc compound	retention time (min)[a]	Re compound	retention time (min)[a]	log *P* of ^{99m}Tc compounds[b]
[^{99m}Tc]**8**	14.2	**9**	13.5	2.55 ± 0.19
[^{99m}Tc]**11**	20.3	**12**	18.4	2.73 ± 0.16
[^{99m}Tc]**14**	9.3	**15**	8.6	1.51 ± 0.09
[^{99m}Tc]**17**	12.4	**18**	11.2	2.51 ± 0.05

[a] Reversed-phase HPLC using a mixture of H_2O/acetonitrile (2/3) as a mobile phase. [b] The measurement was done in triplicate and repeated three times. Each value represents the mean ± SD for three independent experiments.

order: [^{99m}Tc]**11** > [^{99m}Tc]**8** > [^{99m}Tc]**14** > [^{99m}Tc]**17**. ^{99m}Tc complexes (^{99m}Tc-MAMA and ^{99m}Tc-BAT) showed no marked binding to Aβ(1−42) aggregates. This result suggests that the length of the alkyl chain between ^{99m}Tc complexes and the chalcone backbone played an important role in the binding of Aβ(1−42) aggregates, and the difference in ligand (MAMA and BAT) did not affect the affinity.

To confirm the affinity for β-amyloid plaques in the mouse brain, neuropathological fluorescent staining with Re-chalcone derivatives (**9**, **12**, **15**, and **18**) was carried out using Tg2576 mouse brain sections (Figure 3). Many β-amyloid plaques were clearly stained with the derivatives (Figure 3A,C,E,G), as reflected by the high affinity for Aβ aggregates in binding assays *in vitro*, while only minimum labeling was observed in the wild-type mouse brain (Figure 3I). The labeling pattern was consistent with that observed with thioflavin S (Figure 3B,D,F,H). These results suggest that the ^{99m}Tc-chalcones bind to β-amyloid plaques in the mouse brain in addition to having affinity for synthetic Aβ(1−42) aggregates.

Four ^{99m}Tc-labeled chalcones ([^{99m}Tc]**8**, [^{99m}Tc]**11**, [^{99m}Tc]**14**, [^{99m}Tc]**17**) were examined as to their biodistribution in normal mice (Table 2). A biodistribution study provides important information on brain uptake. The ideal β-amyloid imaging probe should have good blood−brain barrier penetration to deliver a sufficient dose into the brain while achieving rapid clearance from normal regions to result in a higher signal-to-noise ratio in the AD brain. Previous studies suggested that the

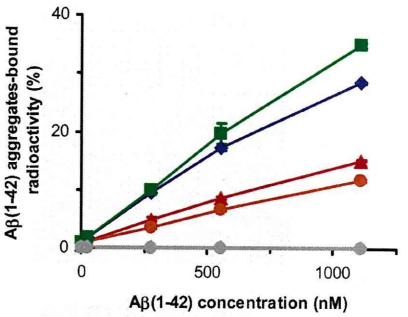

Figure 2. Binding assay of ^{99m}Tc-labeled chalcone derivatives (◆, blue) [^{99m}Tc]**8**, (■) [^{99m}Tc]**11**, (▲) [^{99m}Tc]**14**, (●, orange) [^{99m}Tc]**17**, (●, gray) ^{99m}Tc-MAMA, (◆, gray) ^{99m}Tc-BAT with Aβ(1−42) aggregates. Values are the mean ± standard error of the mean for three independent experiments.

optimal lipophilicity for entry into the brain is obtained with log *P* values of between 1 and 3 (*27*). All four ligands examined in the present study displayed optimal lipophilicity as reflected by their log *P* values (Table 1). Among the four ^{99m}Tc-labeled chalcones, [^{99m}Tc]**17** showed the highest uptake (1.48% ID/g at 2 min postinjection), but [^{99m}Tc]**8**, [^{99m}Tc]**11**, and [^{99m}Tc]**14** did not show sufficient uptake (0.32−0.78% ID/g at 2 min postinjection) despite their lipophilicity. The reason for the low uptake remains unknown. The uptake of [^{99m}Tc]**17** was greater than that of ^{99m}Tc-labeled Aβ imaging agents reported previously, supporting the feasibility of developing ^{99m}Tc-labeled probes for the detection of β-amyloid plaques *in vivo*. Thereafter, the radioactivity of [^{99m}Tc]**17** that accumulated in the brain was rapidly eliminated (0.17% ID/g at 60 min postinjection), a highly desirable property for imaging agents. The pharmacokinetics of [^{99m}Tc]**17** in the brain appears superior to that of any other ^{99m}Tc-labeled probe reported previously, indicating that this chalcone should be investigated further for the imaging of β-amyloid. [^{99m}Tc]**8**, [^{99m}Tc]**11**, and [^{99m}Tc]**14** showed no marked initial uptake, 0.32−0.78% ID/g, and were washed out from the brain relatively slowly (0.11−0.16% ID/g at 60 min). The uptake of [^{99m}Tc]**8**, [^{99m}Tc]**11**, and [^{99m}Tc]**14** appears insufficient for the imaging of β-amyloid plaques in the brain, and additional structural changes are needed to further improve the properties of these chalcone derivatives.

In conclusion, we successfully designed and synthesized novel chalcone derivatives conjugated with ^{99m}Tc or Re complexes for the detection of β-amyloid plaques in the brain. When *in vitro* plaque labeling was carried out using sections of brain from Tg2576 mice, four Re-chalcones intensely stained β-amyloid plaques. In addition, [^{99m}Tc]**17** displayed good uptake into and a rapid washout from the brain after its injection into normal mice. The combination of affinity for β-amyloid plaques, good uptake, and rapid

DOI: 10.1021/cn100042d | ACS Chem. Neurosci. (2010), 1, 598–607

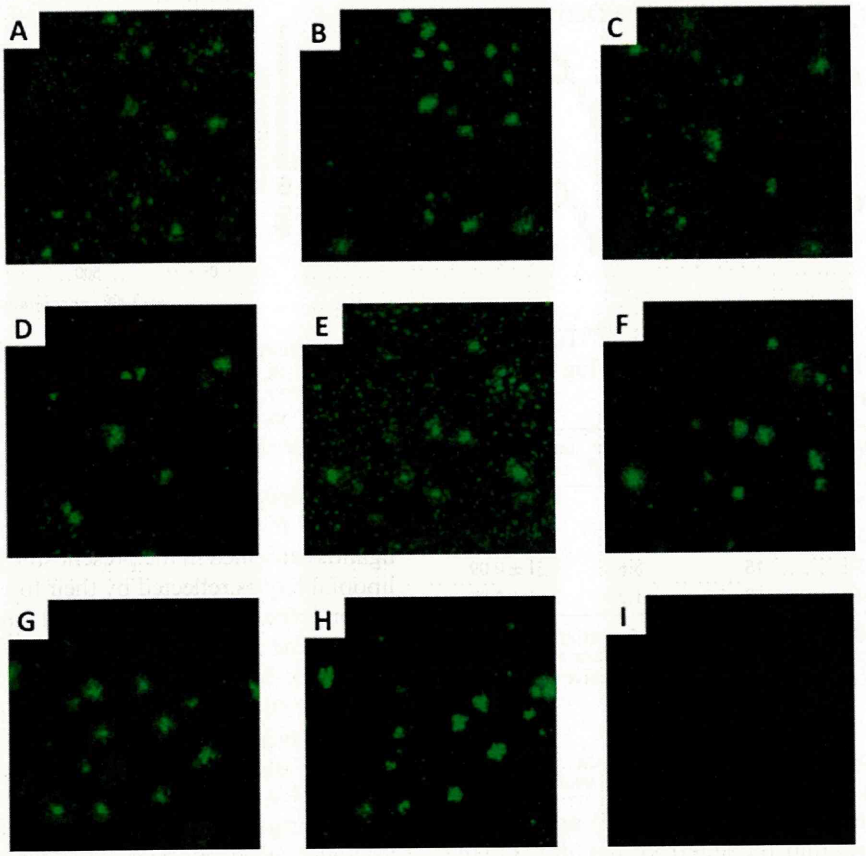

Figure 3. Fluorescent staining of chalcone derivatives **9** (A), **12** (C), **15** (E), and **18** (G) in 10-μm Tg2576 mouse brain sections. Labeled plaques were confirmed by staining of the adjacent sections with thioflavin-S (B, D, F, H). No apparent staining of **18** (I) was observed in the age-matched control mouse brain section.

clearance makes [^{99m}Tc]**17** a promising probe for the detection of β-amyloid plaques in the brain. The results of the present study should provide information useful to the development of ^{99m}Tc-labeled probes for the imaging of β-amyloid plaques in the brain.

Methods

General

All reagents were obtained commercially and used without further purification unless otherwise indicated. ^{1}H NMR spectra were obtained on a Varian Gemini 300 spectrometer with TMS as an internal standard. Coupling constants are reported in hertz. Multiplicity was defined by s (singlet), d (doublet), t (triplet), q (quartet), quin (quintet), and m (multiplet). Mass spectra were obtained on a JEOL IMS-DX. HPLC was performed with a Shimadzu system (a LC-10AT pump with a SPD-10A UV detector, λ = 254 nm) using a Cosmosil C18 column (Nakalai Tesque, 5C18-AR-II, 4.6 mm × 150 mm) and acetonitrile/H_2O (3/2) as the mobile phase at a flow rate of 1.0 mL/min. All key compounds were proven by this method to show >95% purity.

Chemistry

2-(Tritylthio)ethanamine Hydrochloride (1). A solution of 2-mercaptoethylamine hydrochloride (1.14 g, 10 mmol) and triphenylmethyl chloride (2.79 g, 10 mmol) in DMF (10 mL) was stirred at room temperature for 72 h. After the evaporation of DMF, the residue was redissolved in ethyl acetate and added to a 5% $NaHCO_3$ solution in an ice bath. The white precipitate that formed was filtered to yield **1** (3.50 g, 98% yield). ^{1}H NMR (300 MHz, $CDCl_3$) δ 2.31 (t, J = 6.8 Hz, 2H), 2.60 (t, J = 6.8 Hz, 2H), 7.18−7.31 (m, 9H), 7.43 (d, J = 7.2 Hz, 6H).

2-(2-(Tritylthio)ethylamino)-*N*-(2-(tritylthio)ethyl)acetamide (Tr-MAMA) (2). To a stirring solution of **1** (2.50 g, 7.02 mmol) in $CHCl_3$ (20 mL) and triethylamine (5 mL) was slowly added bromoacetyl bromide (0.5 mL, 5.76 mmol) in an ice bath, and the mixture was stirred at 0 °C for 3 h. The mixture was washed with a diluted H_2SO_4 (pH 3), a saturated $NaHCO_3$, and a saturated NaCl solution, sequentially. The organic layers were combined and dried with Na_2SO_4. Evaporation of the solvent gave a residue, which was purified by silica gel chromatography using $CHCl_3$ and then ethyl acetate to give 1.39 g of **2** (58% yield). ^{1}H NMR (300 MHz, $CDCl_3$) δ 2.35 (q, J = 6.6 Hz, 4H), 2.45 (t, J = 5.9 Hz, 2H), 3.02 (s, 2H), 3.07 (q, J = 6.3 Hz, 2H), 7.18−7.29 (m, 18H), 7.38−7.42 (m, 12H). MS m/z 679 (MH^+).

DOI: 10.1021/cn100042d | ACS Chem. Neurosci. (2010), 1, 598–607

Table 2. Biodistribution of Radioactivity after Injection of ^{99m}Tc-Labeled Chalcone Derivatives in Normal Mice[a]

organ	time after injection (min)			
	2	10	30	60
		[^{99m}Tc]**8**		
blood	1.85(0.31)	0.91(0.15)	0.62(0.16)	0.28(0.02)
liver	18.92(2.03)	24.48(1.34)	26.63(5.57)	17.05(1.52)
kidney	9.45(1.24)	7.62(3.79)	9.85(1.35)	5.25(0.87)
intestine[b]	4.71(0.63)	12.45(2.90)	34.90(3.01)	36.49(6.04)
spleen	4.16(0.52)	3.17(0.52)	2.37(0.48)	1.28(0.09)
lung	16.13(1.34)	6.59(1.23)	3.61(1.00)	1.44(0.17)
stomach[b]	0.76(0.10)	1.31(0.15)	2.06(0.65)	1.67(0.29)
pancreas	3.78(0.49)	5.28(0.33)	4.71(0.96)	2.27(0.14)
heart	11.05(1.99)	5.10(1.00)	2.16(0.63)	0.87(0.22)
brain	0.22(0.05)	0.32(0.14)	0.19(0.030)	0.11(0.01)
		[^{99m}Tc]**11**		
blood	2.49(0.24)	0.92(0.05)	0.50(0.11)	0.35(0.13)
liver	23.89(2.51)	24.03(4.51)	23.18(3.67)	21.95(4.58)
kidney	11.26(0.62)	9.66(0.58)	7.64(0.88)	6.39(1.51)
intestine[b]	6.27(0.31)	15.99(0.87)	37.18(2.54)	54.09(10.94)
spleen	3.15(0.22)	1.64(0.33)	0.69(0.16)	0.35(0.15)
lung	15.71(4.59)	4.54(0.57)	1.89(0.24)	1.28(0.49)
stomach[b]	0.95(0.14)	1.37(0.19)	1.77(0.62)	2.41(0.99)
pancreas	4.93(0.87)	3.94(0.84)	1.71(0.30)	0.80(0.32)
heart	13.17(1.42)	3.03(0.36)	1.30(0.35)	0.78(0.10)
brain	0.78(0.16)	0.55(0.06)	0.28(0.09)	0.16(0.09)
		[^{99m}Tc]**14**		
blood	7.84(2.85)	5.37(2.42)	1.55(0.62)	0.41(0.19)
liver	18.35(1.93)	24.89(2.27)	21.29(3.34)	12.96(3.14)
kidney	10.50(1.36)	11.03(2.66)	9.62(1.54)	4.65(0.75)
intestine[b]	3.70(0.55)	9.60(1.35)	31.67(4.85)	41.40(8.54)
spleen	5.87(2.07)	4.44(0.69)	2.71(0.92)	1.42(0.85)
lung	16.33(4.74)	7.87(1.60)	3.16(0.68)	4.12(4.25)
stomach[b]	0.85(0.21)	1.42(0.28)	2.29(0.61)	2.32(0.81)
pancreas	3.14(1.32)	5.30(2.14)	4.64(0.76)	1.63(0.37)
heart	13.26(2.46)	4.96(1.83)	2.54(0.56)	1.23(0.28)
brain	0.62(0.27)	0.47(0.13)	0.38(0.11)	0.16(0.08)
		[^{99m}Tc]**17**		
blood	2.81(0.76)	0.95(0.45)	0.56(0.30)	0.29(0.13)
liver	21.26(2.50)	27.33(2.45)	22.08(3.93)	14.34(0.60)
kidney	11.21(1.46)	8.54(0.64)	4.18(0.52)	1.92(0.41)
intestine[b]	6.22(0.40)	21.95(2.50)	42.24(3.78)	53.39(4.78)
spleen	2.91(0.61)	2.37(0.55)	0.74(0.16)	0.30(0.04)
lung	10.33(1.80)	5.92(1.38)	2.47(0.62)	0.73(0.27)
stomach[b]	1.14(0.26)	1.80(0.22)	1.93(0.19)	1.68(0.67)
pancreas	6.91(2.23)	4.45(0.54)	1.44(0.33)	0.47(0.06)
heart	11.71(2.13)	3.01(0.70)	0.98(0.26)	0.44(0.10)
brain	1.48(0.44)	1.09(0.20)	0.35(0.14)	0.17(0.06)

[a] Each value represents the mean (SD) for 3−6 mice at each interval. Expressed as % injected dose per gram. [b] Expressed as % injected dose per organ.

***tert*-Butyl-2-(2-(tritylthio)ethylamino)ethyl-2-(tritylthio)ethylcarbamate (Tr-BAT) (3).** To a solution of N^1,N^2-bis(2-(tritylthio)ethyl)ethane-1,2-diamine (3.33 g, 5 mmol) and DIPEA (0.86 mL, 5 mmol) in CH_2Cl_2 (80 mL) was added dropwise a solution of $(BOC)_2O$ (1.09 g, 5 mmol) in CH_2Cl_2 (20 mL) in an ice bath. The mixture was stirred at 0 °C for 1 h, concentrated, and purified by column chromatography ($CHCl_3/CH_3OH$ = 99:1) to give 3.59 g of **3** (94%). ^{1}H NMR (300 MHz, $CDCl_3$) δ 1.37 (s, 9H), 1.54 (s, broad, 1H), 2.46−2.28 (m, 8H), 2.96 (s, broad, 4H), 7.17−7.30 (m, 18H), 7.37−7.43 (m, 12H).

(*E*)-3-(4-(Dimethylamino)phenyl)-1-(4-hydroxyphenyl)prop-2-en-1-one (4). *p*-Hydroxyacetophenone (1.36 g, 10 mmol) and *p*-dimethylaminobenzaldehyde (1.49 g, 10 mmol) were dissolved in EtOH (15 mL). A 30-mL aliquot of a 10% aqueous KOH solution was then slowly added dropwise to the reaction mixture. The mixture was stirred for 12 h at 100 °C and then poured into a 1 M aqueous HCl solution and extracted with ethyl acetate. The organic layers were combined and dried over Na_2SO_4. Evaporation of the solvent afforded a residue, which was purified by silica gel chromatography ($CHCl_3/CH_3OH$ = 49:1) to give 1.86 g of **4** (70%). ^{1}H NMR (300 MHz, $CDCl_3$) δ 3.05 (s, 6H), 6.70 (d, J = 8.7 Hz, 2H), 6.91 (d, J = 9.0 Hz, 2H), 7.34 (d, J = 15.3 Hz, 1H), 7.55 (d, J = 9.0 Hz, 2H), 7.79 (d, J = 16.2 Hz, 1H), 7.99 (d, J = 9.0 Hz, 2H).

(*E*)-1-(4-(5-Bromopentyloxy)phenyl)-3-(4-(dimethylamino)-phenyl)prop-2-en-1-one (5). To a solution of **4** (1.51 g, 5.64 mmol) in acetonitrile (15 mL) were added 1,5-dibromopentane (1.54 mL, 11.4 mmol) and K_2CO_3 (1.5 g). The reaction mixture was heated to reflux for 4 h. After the acetonitrile was evaporated, the residue was poured into water and extracted with $CHCl_3$. The organic layer was combined and dried with Na_2SO_4. After the mixture was concentrated, the residue was redissolved in DMSO and washed using hexane. The DMSO layer was concentrated and purified by silica gel chromatography using $CHCl_3$ to give 1.48 g of **5** (63% yield). ^{1}H NMR (300 MHz, $CDCl_3$) δ 1.62−1.70 (m, 2H), 1.83−1.90 (m, 2H), 1.91−2.01 (m, 2H), 3.05 (s, 6H), 3.56 (t, J = 6.8 Hz, 2H), 4.06 (t, J = 6.3 Hz, 2H), 6.70 (d, J = 9.0 Hz, 2H), 6.95 (d, J = 8.7 Hz, 2H), 7.36 (d, J = 15.3 Hz, 1H), 7.55 (d, J = 8.7 Hz, 2H), 7.79 (d, J = 15.6 Hz, 1H), 8.02 (d, J = 9.0 Hz, 2H).

(*E*)-1-(4-(3-Bromopropoxy)phenyl)-3-(4-(dimethylamino)-phenyl)prop-2-en-1-one (6). To a solution of **4** (890 mg, 3.33 mmol) in acetonitrile (25 mL) were added 1,3-dibromopropane (0.679 mL, 6.66 mmol) and K_2CO_3 (1.0 g). The reaction mixture was heated to reflux for 4 h. After the acetonitrile was evaporated, the residue was poured into a saturated NaCl solution and extracted with $CHCl_3$. The organic layer was combined and dried with Na_2SO_4. After the mixture was concentrated, the residue was redissolved in DMF and washed using hexane. The DMF layer was concentrated and purified by silica gel chromatography ($CHCl_3/CH_3OH$ = 199:1) to give 981 mg of **6** (73% yield). ^{1}H NMR (300 MHz, $CDCl_3$) δ 2.35 (quin, J = 6.1 Hz, 2H), 3.04 (s, 6H), 3.61 (t, J = 6.5 Hz, 2H), 4.18 (t, J = 5.7 Hz, 2H), 6.69 (d, J = 9.0 Hz, 2H), 6.97 (d, J = 8.7 Hz, 2H), 7.35 (d, J = 15.3 Hz, 1H), 7.55 (d, J = 8.7 Hz, 2H), 7.79 (d, J = 15.6 Hz, 1H), 8.02 (d, J = 9.0 Hz, 2H).

Compound 7 (Tr-MAMA-C5-CH). To a solution of **5** (485 mg, 1.13 mmol) and **2** (830 mg, 1.22 mmol) in DMF (10 mL) was added DIPEA (1 mL). The reaction mixture was heated to reflux

DOI: 10.1021/cn100042d | ACS Chem. Neurosci. (2010), 1, 598–607

for 12 h. After the evaporation of the solvent, water was added. The mixture was extracted with $CHCl_3$. The organic layers were combined and dried with Na_2SO_4. Evaporation of the solvent gave a residue, which was purified by silica gel chromatography ($CHCl_3/CH_3OH$ = 199:1) to give 330 mg of **7** (29% yield). ^1H NMR (300 MHz, $CDCl_3$) δ 1.39 (s, 4H), 1.69−1.71 (m, 2H), 2.27−2.41 (m, 8H), 2.87 (s, 2H), 2.95−3.01 (m, 2H), 3.04 (s, 6H), 3.93 (t, J = 6.5 Hz, 2H), 6.70 (d, J = 9.0 Hz, 2H), 6.89 (d, J = 8.7 Hz, 2H), 7.14−7.27 (m, 18H), 7.32−7.39 (m, 13H), 7.55 (d, J = 9.0 Hz, 2H), 7.79 (d, J = 15.6 Hz, 1H), 7.99 (d, J = 9.0 Hz, 2H). MS m/z 1014 (MH^+).

Compound 8 (MAMA-C5-CH). To a solution of a little **7** in TFA (200 mL) was added triethylsilane (10 mL), and the solution was mixed. The solvent was removed under a stream of nitrogen gas to give **8**. MS m/z 530 (MH^+).

Compound 9 (Re-MAMA-C5-CH). To a solution of **7** (82 mg, 0.081 mmol) in TFA (4 mL) was added triethylsilane (0.2 mL), and the solution was mixed, and then the solvent was removed under a stream of nitrogen gas. The residue was resolved in a mixed solvent (22 mL, CH_2Cl_2/CH_3OH = 10:1), to which were added $(Ph_3P)_2ReOCl_3$ (135 mg, 0.162 mmol) and 1 M sodium acetate in methanol (4 mL). The reaction mixture was heated to reflux for 6 h and, after cooling to room temperature, mixed with ethyl acetate (60 mL) and filtered. Evaporation of the solvent gave a residue, which was purified by silica gel chromatography ($CHCl_3/CH_3OH$ = 49:1) and then RP-HPLC (acetonitrile/H_2O = 4:1) to give 20 mg (35%) of **9**. ^1H NMR (300 MHz, $CDCl_3$) δ 1.60−1.67 (m, 2H), 1.89−1.92 (m, 4H), 2.82−2.91 (m, 1H), 3.05 (s, 6H), 3.14−3.27 (m, 3H), 3.33−3.42 (m, 1H), 3.52−3.65 (m, 1H), 3.95−4.16 (m, 6H), 4.56−4.62 (m, 1H), 4.67 (d, J = 16.5 Hz, 1H), 6.70 (d, J = 8.7 Hz, 2H), 6.95 (d, J = 8.7 Hz, 2H), 7.35 (d, J = 15.6 Hz, 1H), 7.55 (d, J = 9.0 Hz, 2H), 7.79 (d, J = 15.6 Hz, 1H), 8.03 (d, J = 8.7 Hz, 2H). HRMS m/z $C_{28}H_{37}N_3O_4ReS_2$ found 730.1748, calcd 730.1783 (MH^+).

Compound 10 (Tr-BAT-C5-CH). To a solution of **5** (630 mg, 1.51 mmol) and **3** (855 mg, 1.12 mmol) in DMF (20 mL) was added DIPEA (2 mL). The reaction mixture was heated to reflux for 12 h. After the evaporation of the solvent, the residue was purified by silica gel chromatography using $CHCl_3$ and then ethyl acetate/hexane (1:2) to give 126 mg of **10** (10% yield). ^1H NMR (300 MHz, $CDCl_3$) δ 1.32−1.37 (m, 12H), 1.70−1.77 (m, 2H), 2.20−2.35 (m, 10H), 2.85−3.01 (m, 4H), 3.04 (s, 6H), 3.98 (t, J = 6.5 Hz, 2H), 6.69 (d, J = 9.3 Hz, 2H), 6.93 (d, J = 8.7 Hz, 2H), 7.15−7.29 (m, 18H), 7.33−7.42 (m, 13H), 7.55 (d, J = 8.7 Hz, 2H), 7.79 (d, J = 15.6 Hz, 1H), 8.01 (d, J = 9.0 Hz, 2H). MS m/z 1100 (MH^+).

Compound 11 (BAT-C5-CH). To a solution of **10** in TFA (200 mL) was added triethylsilane (10 mL), and the solution was mixed. The solvent was removed under a stream of nitrogen gas to give **11**. MS m/z 516 (MH^+).

Compound 12 (Re-BAT-C5-CH). To a solution of **10** (110 mg, 0.100 mmol) in TFA (4 mL) was added triethylsilane (0.2 mL), and the solution was mixed, and then the solvent was removed under a stream of nitrogen gas. The residue was resolved in a mixed solvent (22 mL, CH_2Cl_2/CH_3OH = 10:1), to which were added $(Ph_3P)_2ReOCl_3$ (167 mg, 0.200 mmol) and 1 M sodium acetate in methanol (4 mL). The reaction mixture was heated to reflux for 6 h and, after cooling to room temperature, mixed with ethyl acetate (60 mL) and filtered. Evaporation of the solvent gave a residue, which was purified by silica gel chromatography ($CHCl_3/CH_3OH$ = 49:1) and then RP-HPLC (acetonitrile/H_2O = 4:1) to give 44 mg (61%) of **12**. ^1H NMR (300 MHz, $CDCl_3$) δ 1.60−1.73 (m, 2H), 1.87−1.92 (m, 4H), 2.72−2.78 (m, 1H), 2.96−3.00 (m, 2H), 3.05 (s, 6H), 3.21−3.41 (m, 4H), 3.53−3.63 (m, 1H), 3.76−3.92 (m, 3H), 4.06−4.17 (m, 5H), 6.70 (d, J = 8.7 Hz, 2H), 6.96 (d, J = 9.0 Hz, 2H), 7.36 (d, J = 15.6 Hz, 1H), 7.56 (d, J = 9.0 Hz, 2H), 7.79 (d, J = 15.6 Hz, 1H), 8.03 (d, J = 9.0 Hz, 2H). HRMS m/z $C_{28}H_{39}N_3O_3ReS_2$ found 716.1990, calcd 716.1990 (MH^+).

Compound 13 (Tr-MAMA-C3-CH). To a solution of **6** (981 mg, 2.53 mmol) and **2** (1.72 g, 2.53 mmol) in DMF (30 mL) was added DIPEA (3 mL). The reaction mixture was heated to reflux for 12 h. After the evaporation of the solvent, water was added. The mixture was extracted with $CHCl_3$. The organic layers were combined and dried with Na_2SO_4. Evaporation of the solvent gave a residue, which was purified by silica gel chromatography (ethyl acetate/hexane = 3:2) to give 714 mg of **13** (29% yield). ^1H NMR (300 MHz, $CDCl_3$) δ 1.80−1.87 (m, 2H), 2.28 (t, J = 6.3 Hz, 2H), 2.33−2.43 (m, 4H), 2.51 (t, J = 6.9 Hz, 2H), 2.91 (s, 2H), 2.99−3.03 (m, 2H), 3.05 (s, 6H), 3.99 (t, J = 5.9 Hz, 2H), 6.70 (d, J = 9.0 Hz, 2H), 6.86 (d, J = 9.0 Hz, 2H), 7.14−7.27 (m, 18H), 7.29−7.38 (m, 13H), 7.54 (d, J = 8.7 Hz, 2H), 7.78 (d, J = 15.3 Hz, 1H), 7.93 (d, J = 9.0 Hz, 2H). MS m/z 986 (MH^+).

Compound 14 (MAMA-C3-CH). To a solution of **13** in TFA (200 mL) was added triethylsilane (10 mL), and the solution was mixed. The solvent was removed under a stream of nitrogen gas to give **14**. MS m/z 502 (MH^+).

Compound 15 (Re-MAMA-C3-CH). To a solution of **13** (99 mg, 0.100 mmol) in TFA (4 mL) was added triethylsilane (0.2 mL), and the solution was mixed, and then the solvent was removed under a stream of nitrogen gas. The residue was resolved in a mixed solvent (22 mL, CH_2Cl_2/CH_3OH = 10:1), to which were added $(Ph_3P)_2ReOCl_3$ (167 mg, 0.200 mmol) and 1 M sodium acetate in methanol (4 mL). The reaction mixture was heated to reflux for 6 h and, after cooling to room temperature, mixed with ethyl acetate (60 mL) and filtered. Evaporation of the solvent gave a residue, which was purified with silica gel chromatography ($CHCl_3/CH_3OH$ = 49:1) and then RP-HPLC (acetonitrile/H_2O = 4:1) to give 20 mg (29%) of **15**. ^1H NMR (300 MHz, $CDCl_3$) δ 1.65−1.75 (m, 1H), 2.32−2.37 (m, 2H), 2.90−2.98 (m, 1H), 3.05 (s, 6H), 3.15−3.34 (m, 3H), 3.40−3.52 (m, 1H), 3.81−3.86 (m, 1H), 4.09−4.19 (m, 5H), 4.58−4.64 (m, 1H), 4.74 (d, J = 16.2 Hz, 1H), 6.70 (d, J = 9.0 Hz, 2H), 6.96 (d, J = 8.7 Hz, 2H), 7.40 (d, J = 15.3 Hz, 1H), 7.56 (d, J = 8.7 Hz, 2H), 7.79 (d, J = 15.3 Hz, 1H), 8.03 (d, J = 9.0 Hz, 2H). HRMS m/z $C_{26}H_{33}N_3O_4ReS_2$ found 702.1476, calcd 702.1470 (MH^+).

Compound 16 (Tr-BAT-C3-CH). To a solution of **6** (243 mg, 0.626 mmol) and **3** (479 mg, 0.626 mmol) in DMF (10 mL) was added DIPEA (1 mL). The reaction mixture was heated to reflux for 12 h. After the evaporation of the solvent, a saturated NaCl solution was added. The mixture was extracted with $CHCl_3$. The organic layers were combined and dried with Na_2SO_4. Evaporation of the solvent gave a residue, which was purified by silica gel chromatography

DOI: 10.1021/cn100042d | ACS Chem. Neurosci. (2010), 1, 598–607

using $CHCl_3$ and then ethyl acetate/hexane (1:2) to give 128 mg of **16** (19% yield). ^{1}H NMR (300 MHz, $CDCl_3$) δ 1.37 (s, 9H), 1.73 (t, J = 6.0 Hz, 2H), 2.24−2.38 (m, 10H), 2.88−2.95 (m, 4H), 3.04 (s, 6H), 3.97 (t, J = 6.2 Hz, 2H), 6.70 (d, J = 9.0 Hz, 2H), 6.89 (d, J = 8.7 Hz, 2H), 7.15−7.31 (m, 19H), 7.37−7.41 (m, 12H), 7.54 (d, J = 9.0 Hz, 2H), 7.78 (d, J = 15.6 Hz, 1H), 7.96 (d, J = 8.7 Hz, 2H). MS m/z 1072 (MH^+).

Compound 17 (BAT-C3-CH). To a solution of **16** in TFA (200 mL) was added triethylsilane (10 mL), and the solution was mixed. The solvent was removed under a stream of nitrogen gas to give **17**. MS m/z 488 (MH^+).

Compound 18 (Re-BAT-C3-CH). To a solution of **16** (104 mg, 0.097 mmol) in TFA (4 mL) was added triethylsilane (0.2 mL), and the solution was mixed, and then the solvent was removed under a stream of nitrogen gas. The residue was resolved in a mixed solvent (22 mL, CH_2Cl_2/CH_3OH = 10:1), to which were added $(Ph_3P)_2ReOCl_3$ (167 mg, 0.200 mmol) and 1 M sodium acetate in methanol (4 mL). The reaction mixture was heated to reflux for 6 h and, after cooling to room temperature, mixed with ethyl acetate (60 mL) and filtered. Evaporation of the solvent gave a residue, which was purified with silica gel chromatography ($CHCl_3/CH_3OH$ = 49:1) and then RP-HPLC (acetonitrile/H_2O = 4:1) to give 44 mg (66%) of **18**. ^{1}H NMR (300 MHz, $CDCl_3$) δ1.75−1.85 (m, 1H), 2.31−2.38 (m, 2H), 2.76−2.82 (m, 1H), 2.91−3.08 (m, 2H), 3.05 (s, 6H), 3.24−3.49 (m, 4H), 3.76−4.00 (m, 3H), 4.12−4.33 (m, 5H), 6.70 (d, J = 9.0 Hz, 2H), 6.95 (d, J = 9.0 Hz, 2H), 7.35 (d, J = 15.3 Hz, 1H), 7.56 (d, J = 9.0 Hz, 2H), 7.79 (d, J = 15.3 Hz, 1H), 8.03 (d, J = 8.7 Hz, 2H). HRMS m/z $C_{26}H_{35}N_3O_3ReS_2$ found 688.1631, calcd 688.1677 (MH^+).

^{99m}Tc Labeling Reaction

To a solution of sodium heptonate dehydrate (2.0 g, 7.04 mmol) in nanopure water (25 mL) was added a 0.75 mL aliquot of a $SnCl_2 \cdot 2H_2O$ solution [12 mg of Tin(II) chloride dehydrate (53.2 mmol) was dissolved in 0.1 M HCl (15 μL)]. This solution was adjusted to pH 8.5−9.0 with a small amount of 0.1 M NaOH and then lyophilized to give tin glucoheptonate (SnGH) kit. SnGH kit (1 mg) was added to a $Na^{99m}TcO_4$ solution (200 μL) and reacted at room temperature for 10 min to give a ^{99m}TcGH solution. To solutions of **7**, **10**, **13**, and **16** (0.5 mg) in TFA (200 μL) was added triethylsilane (10 μL), and the solutions were mixed, and then the solvents were removed under a stream of nitrogen gas. The residues were resolved in acetonitrile (200 μL), to which were added a 0.1 M HCl solution (15 μL) and the ^{99m}TcGH solution (200 mL). The reaction mixtures were heated to 80−90 °C for 10 min. The residue taken up in 100 μL of acetonitrile was purified by a reversed-phase HPLC system with an isocratic solvent of acetonitrile/H_2O (3/2) as the mobile phase at a flow rate of 1.0 mL/min. After cooling to room temperature, the mixtures were purified with RP-HPLC to give [^{99m}Tc]**8**, [^{99m}Tc]**11**, [^{99m}Tc]**14**, and [^{99m}Tc]**17**. The desired fraction was collected in a flask and evaporated dry. The radiochemical identity of [^{99m}Tc]**8**, [^{99m}Tc]**11**, [^{99m}Tc]**14**, and [^{99m}Tc]**17** was verified with the corresponding Re-complex from the HPLC profiles. The final ^{99m}Tc-complexes showed a single peak of radioactivity at retention times of 14.2, 20.3, 9.3, and 12.4 min, respectively, close to those of the Re complexes. The four ^{99m}Tc-complexes were obtained in 46−95% radiochemical yields with a radiochemical purity of >95% after HPLC.

Partition Coefficient

Partition coefficients were measured by mixing the [^{99m}Tc]tracer with 3 mL each of 1-octanol and buffer (0.1 M phosphate, pH 7.4) in a test tube. The test tube was vortexed for 3 min at room temperature, then centrifuged for 5 min. Two weighed samples (0.5 mL) from the 1-octanol and buffer layers were measured in a well counter. The partition coefficient was determined by calculating the ratio of counts per minute per gram of 1-octanol to that of buffer. Samples from the 1-octanol layer were repartitioned until consistent partitions of coefficient values were obtained. The measurement was done in triplicate and repeated three times.

Binding Assays Using the Aggregated Aβ Peptides in Solution

A solid form of Aβ(1−42) was purchased from Peptide Institute (Osaka, Japan). Aggregation was carried out by gently dissolving the peptide (0.25 mg/mL) in a buffer solution (pH 7.4) containing 10 mM sodium phosphate and 1 mM EDTA. The solutions were incubated at 37 °C for 42 h with gentle and constant shaking. The binding assay was performed by mixing 50 μL of Aβ(1−42) aggregates (0−100 μg/mL), 50 μL of an appropriate concentration of the ^{99m}Tc-labeled form ([^{99m}Tc]**8**, [^{99m}Tc]**11**, [^{99m}Tc]**14**, [^{99m}Tc]**17**), and 900 μL of 30% ethanol in 12 mm × 75 mm borosilicate glass tubes. Nonspecific binding was defined in the presence of 1 μM of chalcone derivative (4-dimethylamino-4′-iodo-chalcone) (*20*). After incubation for 3 h at room temperature, the mixture was filtered through GF/B filters (Whatman, Kent, U.K.) using an M-24 cell harvester (Brandel, Gaithersburg, MD). Filters containing the bound ^{99m}Tc-labeled form were examined in a γ counter (Perkin-Elmer, WIZARD^2 2470).

Biodistribution in Normal Mice

The experiments with animals were conducted in accordance with our institutional guidelines and approved by the Nagasaki University Animal Care Committee. A saline solution (100 μL) of ^{99m}Tc-chalcones (1.0×10^7 cpm/mL) containing ethanol (30 μL) was injected intravenously directly into the tail of ddY mice (5 weeks old, 22−25 g). The mice were sacrificed at various time points postinjection. The organs of interest were removed and weighed, and radioactivity was measured with an automatic γ counter (Perkin-Elmer, WIZARD^2 2470).

Neuropathological Staining of Mouse Brain Sections

The Tg2576 transgenic (female, 30-month-old) and wild-type mice (female, 30-month-old) mice were used as the Alzheimer's model and control, respectively. After the mice were sacrificed by decapitation, the brains were immediately removed and frozen in powdered dry ice. The frozen blocks were sliced into serial sections, 10 μm thick. Each slide was incubated with a 50% EtOH solution (2.5−10 μM) of **9**, **12**, **15**, and **18** for 2−9 h. The sections were washed in 50% EtOH for 5 min two times and examined for **9**, **12**, **15**, and **18** with excitation of 458 nm using a microscope (Carl Zeiss, LSM710). Thereafter, the serial sections were also stained with thioflavin S, a pathological dye commonly used for staining β-amyloid plaques in the brain.

DOI: 10.1021/cn100042d | ACS Chem. Neurosci. (2010), 1, 598–607

Author Information

Corresponding Author

*For M. Ono: phone +81-75-753-4608, fax +81-75-753-4568, e-mail ono@pharm.kyoto-u.ac.jp. For M. Nakayama: phone +81-95-819-2441, fax +81-95-819-2441, e-mail morio@nagasaki-u.ac.jp.

Funding Sources

This study was supported by the Program for Promotion of Fundamental Studies in Health Sciences of the National Institute of Biomedical Innovation (NIBIO), a Health Labour Sciences Research Grant, and a Grant-in-aid for Young Scientists (A) and Exploratory Research from the Ministry of Education, Culture, Sports, Science and Technology, Japan.

References

1. Selkoe, D. J. (2001) Alzheimer's disease: Genes, proteins, and therapy. *Physiol. Rev. 81*, 741–766.

2. Selkoe, D. J. (2000) Imaging Alzheimer's amyloid. *Nat. Biotechnol. 18*, 823–824.

3. Mathis, C. A., Wang, Y., and Klunk, W. E. (2004) Imaging β-amyloid plaques and neurofibrillary tangles in the aging human brain. *Curr. Pharm. Des. 10*, 1469–1492.

4. Nordberg, A. (2004) PET imaging of amyloid in Alzheimer's disease. *Lancet Neurol. 3*, 519–527.

5. Mathis, C. A., Wang, Y., Holt, D. P., Huang, G. F., Debnath, M. L., and Klunk, W. E. (2003) Synthesis and evaluation of ^{11}C-labeled 6-substituted 2-arylbenzothiazoles as amyloid imaging agents. *J. Med. Chem. 46*, 2740–2754.

6. Klunk, W. E., Engler, H., Nordberg, A., Wang, Y., Blomqvist, G., Holt, D. P., Bergstrom, M., Savitcheva, I., Huang, G. F., Estrada, S., Ausen, B., Debnath, M. L., Barletta, J., Price, J. C., Sandell, J., Lopresti, B. J., Wall, A., Koivisto, P., Antoni, G., Mathis, C. A., and Langstrom, B. (2004) Imaging brain amyloid in Alzheimer's disease with Pittsburgh Compound-B. *Ann. Neurol. 55*, 306–319.

7. Ono, M., Wilson, A., Nobrega, J., Westaway, D., Verhoeff, P., Zhuang, Z. P., Kung, M. P., and Kung, H. F. (2003) ^{11}C-Labeled stilbene derivatives as Aβ-aggregate-specific PET imaging agents for Alzheimer's disease. *Nucl. Med. Biol. 30*, 565–571.

8. Verhoeff, N. P., Wilson, A. A., Takeshita, S., Trop, L., Hussey, D., Singh, K., Kung, H. F., Kung, M. P., and Houle, S. (2004) In-vivo imaging of Alzheimer disease β-amyloid with [^{11}C]SB-13 PET. *Am. J. Geriatr. Psychiatry 12*, 584–595.

9. Zhang, W., Oya, S., Kung, M. P., Hou, C., Maier, D. L., and Kung, H. F. (2005) F-18 polyethyleneglycol stilbenes as PET imaging agents targeting Aβ aggregates in the brain. *Nucl. Med. Biol. 32*, 799–809.

10. Rowe, C. C., Ackerman, U., Browne, W., Mulligan, R., Pike, K. L., O'Keefe, G., Tochon-Danguy, H., Chan, G., Berlangieri, S. U., Jones, G., Dickinson-Rowe, K. L., Kung, H. P., Zhang, W., Kung, M. P., Skovronsky, D., Dyrks, T., Holl, G., Krause, S., Friebe, M., Lehman, L., Lindemann, S., Dinkelborg, L. M., Masters, C. L., and Villemagne, V. L. (2008) Imaging of amyloid β in Alzheimer's disease with ^{18}F-BAY94-9172, a novel PET tracer: proof of mechanism. *Lancet Neurol. 7*, 129–135.

11. Kudo, Y., Okamura, N., Furumoto, S., Tashiro, M., Furukawa, K., Maruyama, M., Itoh, M., Iwata, R., Yanai, K., and Arai, H. (2007) 2-(2-[2-Dimethylaminothiazol-5-yl]ethenyl)-6-(2-[fluoro]ethoxy)benzoxazole: A novel PET agent for *in vivo* detection of dense amyloid plaques in Alzheimer's disease patients. *J. Nucl. Med. 48*, 553–561.

12. Agdeppa, E. D., Kepe, V., Liu, J., Flores-Torres, S., Satyamurthy, N., Petric, A., Cole, G. M., Small, G. W., Huang, S. C., and Barrio, J. R. (2001) Binding characteristics of radiofluorinated 6-dialkylamino-2-naphthylethylidene derivatives as positron emission tomography imaging probes for β-amyloid plaques in Alzheimer's disease. *J. Neurosci. 21*, No. RC189.

13. Shoghi-Jadid, K., Small, G. W., Agdeppa, E. D., Kepe, V., Ercoli, L. M., Siddarth, P., Read, S., Satyamurthy, N., Petric, A., Huang, S. C., and Barrio, J. R. (2002) Localization of neurofibrillary tangles and β-amyloid plaques in the brains of living patients with Alzheimer disease. *Am. J. Geriatr. Psychiatry 10*, 24–35.

14. Kung, M. P., Hou, C., Zhuang, Z. P., Zhang, B., Skovronsky, D., Trojanowski, J. Q., Lee, V. M., and Kung, H. F. (2002) IMPY: An improved thioflavin-T derivative for *in vivo* labeling of β-amyloid plaques. *Brain Res. 956*, 202–210.

15. Zhuang, Z. P., Kung, M. P., Wilson, A., Lee, C. W., Plossl, K., Hou, C., Holtzman, D. M., and Kung, H. F. (2003) Structure–activity relationship of imidazo[1,2-*a*]pyridines as ligands for detecting β-amyloid plaques in the brain. *J. Med. Chem. 46*, 237–243.

16. Newberg, A. B., Wintering, N. A., Clark, C. M., Plossl, K., Skovronsky, D., Seibyl, J. P., Kung, M. P., and Kung, H. F. (2006) Use of ^{123}I IMPY SPECT to differentiate Alzheimer's disease from controls. *J. Nucl. Med. 47*, 78P.

17. Zhang, W., Kung, M. P., Oya, S., Hou, C., and Kung, H. F. (2007) ^{18}F-labeled styrylpyridines as PET agents for amyloid plaque imaging. *Nucl. Med. Biol. 34*, 89–97.

18. Choi, S. R., Golding, G., Zhuang, Z., Zhang, W., Lim, N., Hefti, F., Benedum, T. E., Kilbourn, M. R., Skovronsky, D., and Kung, H. F. (2009) Preclinical properties of ^{18}F-AV-45: A PET agent for Aβ plaques in the brain. *J. Nucl. Med. 50*, 1887–1894.

19. Ono, M., Haratake, M., Mori, H., and Nakayama, M. (2007) Novel chalcones as probes for *in vivo* imaging of β-amyloid plaques in Alzheimer's brains. *Bioorg. Med. Chem. 15*, 6802–6809.

20. Ono, M., Hori, M., Haratake, M., Tomiyama, T., Mori, H., and Nakayama, M. (2007) Structure-activity relationship of chalcones and related derivatives as ligands for detecting of β-amyloid plaques in the brain. *Bioorg. Med. Chem. 15*, 6388–6396.

21. Ono, M., Watanabe, R., Kawashima, H., Cheng, Y., Kimura, H., Watanabe, H., Haratake, M., Saji, H., and Nakayama, M. (2009) Fluoro-pegylated chalcones as positron emission tomography probes for *in vivo* imaging of β-amyloid plaques in Alzheimer's disease. *J. Med. Chem. 52*, 6394–6401.

22. Han, H., Cho, C. G., and Lansbury, P. T., Jr. (1996) Technetium complexes for the quantitation of brain amyloid. *J. Am. Chem. Soc. 118*, 4506–4507.

23. Dezutter, N. A., Dom, R. J., de Groot, T. J., Bormans, G. M., and Verbruggen, A. M. (1999) ^{99m}Tc-MAMA-chrysamine G, a probe for β-amyloid protein of Alzheimer's disease. *Eur. J. Nucl. Med. 26*, 1392–1399.

24. Chen, X., Yu, P., Zhang, L., and Liu, B. (2008) Synthesis and biological evaluation of ^{99m}Tc, Re-monoamine-monoamide conjugated to 2-(4-aminophenyl)benzothiazole as potential probes for β-amyloid plaques in the brain. *Bioorg. Med. Chem. Lett. 18*, 1442–1445.

25. Serdons, K., Verduyckt, T., Cleynhens, J., Terwinghe, C., Mortelmans, L., Bormans, G., and Verbruggen, A. (2007) Synthesis and evaluation of a ^{99m}Tc-BAT-phenylbenzothiazole conjugate as a potential *in vivo* tracer for visualization of amyloid β. *Bioorg. Med. Chem. Lett. 17*, 6086–6090.

26. Oya, S., Plossl, K., Kung, M. P., Stevenson, D. A., and Kung, H. F. (1998) Small and neutral Tc(v)O BAT, bisaminoethanethiol (N2S2) complexes for developing new brain imaging agents. *Nucl. Med. Biol. 25*, 135–140.

27. Dishino, D. D., Welch, M. J., Kilbourn, M. R., and Raichle, M. E. (1983) Relationship between lipophilicity and brain extraction of C-11-labeled radiopharmaceuticals. *J. Nucl. Med. 24*, 1030–1038.

Note Added after ASAP Publication

This paper was published on the Web on July 8, 2010, with an error in Figure 3. The corrected version was reposted on July 13, 2010.

DOI: 10.1021/cn100042d | *ACS Chem. Neurosci.* (2010), *1*, 598–607

ACS Medicinal Chemistry Letters

pubs.acs.org/acsmedchemlett

Fluorinated Benzofuran Derivatives for PET Imaging of β-Amyloid Plaques in Alzheimer's Disease Brains

Yan Cheng,[†] Masahiro Ono,*[,†] Hiroyuki Kimura,[†] Shinya Kagawa,[‡] Ryuichi Nishii,[‡] Hidekazu Kawashima,[†] and Hideo Saji*[,†]

[†]Department of Patho-Functional Bioanalysis, Graduate School of Pharmaceutical Sciences, Kyoto University, Yoshida Shimoadachi-cho, Sakyo-ku, Kyoto 606-8501, Japan, and [‡]Shiga Medical Center Research Institute, 5-4-30, Moriyama, Moriyama City, Shiga, 524-8524, Japan

ABSTRACT A series of fluorinated benzofuran derivatives as potential tracers for positron emission tomography (PET) targeting β-amyloid plaques in the brains of patients with Alzheimer's disease (AD) were synthesized and evaluated. The derivatives were produced using an intramolecular Wittig reaction. In experiments in vitro, all displayed high affinity for Aβ(1−42) aggregates with K_i values in the nanomolar range. Radiofluorinated **17**, [^{18}F]**17**, in particular labeled β-amyloid plaques in sections of Tg2576 mouse brain and displayed high uptake (5.66% ID/g) at 10 min postinjection, sufficient for PET imaging. In addition, in vivo β-amyloid plaque labeling can be clearly demonstrated with [^{18}F]**17** in Tg2576 mice. In conclusion, [^{18}F]**17** may be useful for detecting β-amyloid plaques in patients with AD.

KEYWORDS Alzheimer's disease, fluorine-18, benzofuran, positron emission tomography (PET)

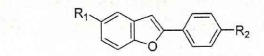

compounds	R_1	R_2
5	F	NH_2
6	F	$NHCH_3$
7	F	$N(CH_3)_2$
17	$F(CH_2CH_2O)_3$	$N(CH_3)_2$
21		$N(CH_3)_2$

Alzheimer's disease (AD) is a neurodegenerative disorder characterized by dementia, cognitive impairment, and memory loss. Autopsied brains of AD patients show neuropathological features such as the presence of senile plaques and neurofibrillary tangles, which contain β-amyloid peptides (Aβ) and highly phosphorylated τ proteins. Aβ aggregates in the brain are a hallmark of AD.[1,2] The quantitative evaluation of Aβ aggregates in the brain with noninvasive techniques such as positron emission tomography (PET) and single photon emission computed tomography (SPECT) would allow a presymptomatic diagnosis and the monitoring of putative effects of neuroprotective treatments. Thus, great efforts have been made to develop radiotracers that bind to β-amyloid plaques in vivo.[3−5]

Recent success in developing radiolabeled agents targeting Aβ aggregates has provided a window of opportunity to improve the diagnosis of AD. Preliminary reports of PET imaging suggested that [^{11}C]4-*N*-methylamino-4′-hydroxystilbene (SB-13),[6] [^{11}C]2-(4′-(methylaminophenyl)-6-hydroxybenzothiazole (PIB),[7,8] and [^{11}C]2-(2-[2-dimethylaminothiazol-5-yl]ethenyl)-6-(2-[fluoro]ethoxy)benzoxazole (BF-227)[9] showed differential uptake and retention in the brain of AD patients as compared to controls. However, ^{11}C is a positron-emitting isotope with a short $t_{1/2}$ (20 min), which limits its clinical application. Recent efforts have focused on the development of comparable agents labeled with a longer half-life isotope, ^{18}F ($t_{1/2}$, 110 min). Preliminary studies with [^{18}F]-2-(1-(2-(*N*-(2-fluoroethyl)-*N*-methylamino)-naphthalene-6-yl)ethylidene)malononitrile ([^{18}F]FDDNP)[10,11] showed differential uptake and retention in the brain of AD patients for the first time. More recently, a stilbene derivative, [^{18}F]BAY94-9172,[12,13] and a styrylpyridine derivative, [^{18}F]AV-45,[14,15] and a fluorinated PIB analogue, [^{18}F]GE-067,[16] have proven useful in the imaging of β-amyloid plaques in living human brain tissue in clinical trials (Figure 1).

To search for more candidates for ^{18}F-labeled tracers for PET, we planned to evaluate a new series of benzofuran derivatives previously reported as useful radioiodinated or ^{11}C-labeled probes for imaging β-amyloid plaques.[17,18] The derivatives showed good affinity for Aβ aggregates in vitro in binding experiments using synthetic Aβ aggregates and neuropathological staining of AD brain sections. We report here the in vitro and in vivo evaluation of a series of fluorinated benzofuran derivatives as probes for imaging β-amyloid plaques by PET.

The synthesis of the fluorinated benzofuran derivatives is outlined in Schemes 1−3. The key step in the formation of the benzofuran backbone is accomplished by an intramolecular Wittig reaction between triphenyl phosphonium salt and 4-nitrobenzoyl chloride or 4-dimethylaminobenzoyl chloride.[17] The desired Wittig reagent, **3**, was readily prepared from 5-fluoro-2-hydroxybenzyl alcohol and triphenylphosphine hydrobromide (yield 71%). Another Wittig reagent, **13**, was readily prepared from 2-hydroxy-5-methoxybenzyl alcohol and triphenylphosphine hydrobromide (yield 84%). Wittig reactions afforded the desired benzofurans (**4**, **7**, and **14**) in yields of 31, 55, and 27%, respectively.

Received Date: April 19, 2010
Accepted Date: June 30, 2010
Published on Web Date: July 11, 2010

ACS Medicinal Chemistry Letters
pubs.acs.org/acsmedchemlett

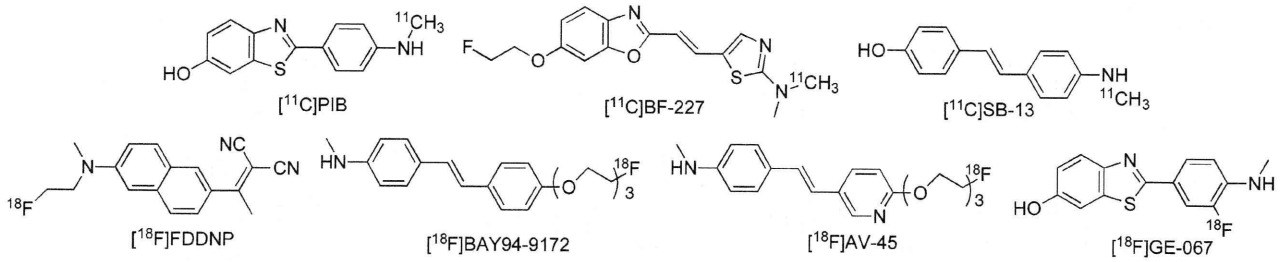

Figure 1. Chemical structures of PET imaging agents targeting β-amyloid plaques in AD patients.

Scheme 1[a]

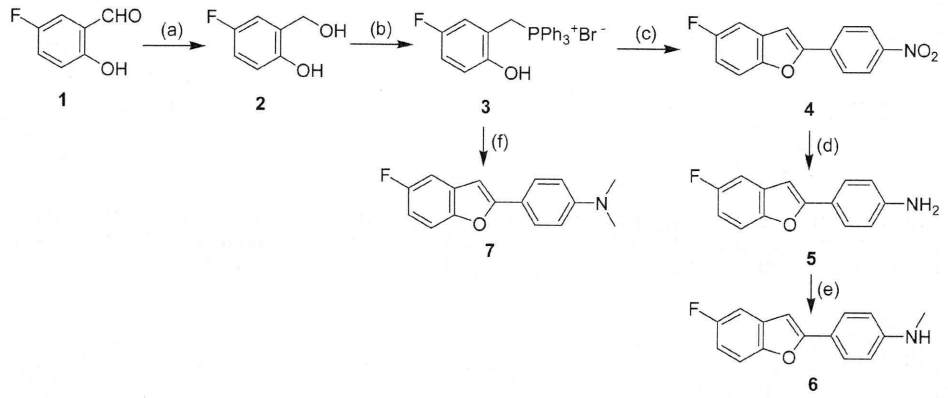

[a] Reagents and conditions: (a) $NaBH_4$, ethanol. (b) Triphenylphosphine hydrobromide, acetonitrile, reflux. (c) 4-Nitrobenzoyl chloride, toluene/NEt_3, reflux. (d) $SnCl_2$, ethanol, reflux. (e) $(CH_2O)_n$, NaOMe, methanol, reflux. $NaBH_4$, reflux. (f) 4-Dimethylaminobenzoyl chloride, toluene/NEt_3, reflux.

Scheme 2[a]

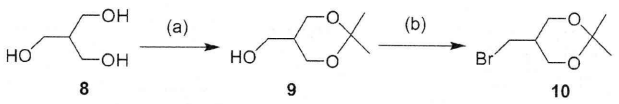

[a] Reagents and conditions: (a) $(CH_3O)_2C(CH_3)_2$, TsOH. (b) CBr_4, PPh_3, pyridine, DCM.

To prepare the amine compound **5**, the nitro group was reduced with $SnCl_2$ in ethanol (yield 93%). Conversion of **5** to the corresponding monomethylamino derivative **6** was achieved by monomethylation with paraformaldehyde and NaOMe (yield 30%). The synthesis outlined in Schemes 2 and 3 was achieved using methods reported previously.[18−22]

The binding experiments were carried out as described previously.[17,23] Assays using Aβ(1−42) aggregates demonstrated that these fluorinated benzofuran derivatives competed with [^{125}I]IMPY to bind β-amyloid plaques with excellent affinity (Table 1).[24,25] Compound **7** with a dimethylaminophenyl moiety in the phenylbenzofuran molecule displayed slightly lower values (higher affinity) than **5** with an aminophenyl moiety or **6** with a monomethylaminophenyl moiety. However, all of the derivatives maintained good binding affinity with K_i values in the nanomolar range. The results strongly support our previous finding that benzofuran derivatives have considerable tolerance for structural modification.[17,18] Among the derivatives with high affinity for Aβ aggregates, **17** was tested further because of the ease with which it could be labeled with ^{18}F.

The ^{18}F-labeled **17** ([^{18}F]**17**) was prepared from a tosyl precursor (**22**) via a nucleophilic displacement reaction with the fluoride anion (Scheme 4).[23] A solution of **22** (1.0 mg) in acetonitrile (200 μL) was added to a reaction vessel containing ^{18}F. The mixture was heated at 120 °C for 10 min. Radiolabeling of the precursor generated [^{18}F]**17** with an average radiochemical yield of 10.0% and radiochemical purity of >99%. The specific activity of [^{18}F]**17** was 242 GBq/μmol. The identity of [^{18}F]**17** was verified by a comparison of the retention time with the nonradioactive compound. Initially, **21** was expected to show similar radiolabeling to **17**. However, the radiolabeling of **21** under the various reaction conditions normally used for ^{18}F radiolabeling gave a radiochemical yield (<0.1%) too low to conduct a subsequent distribution experiment.

To evaluate the uptake of [^{18}F]**17** in the brain, a biodistribution experiment was performed in normal mice (Table 2). [^{18}F]**17** displayed high uptake (5.66% ID/g) at 10 min postinjection, sufficient for PET imaging, and the radioactivity in the brain cleared with time. At 60 min postinjection, the uptake was 2.80% ID/g, indicating a relatively slow washout from the brain. One way to select a ligand with appropriate kinetics in vivo is to use the $\text{brain}_{2\text{ min}}/\text{brain}_{60\text{ min}}$ ratio as an index to compare the washout rate. Although the $\text{brain}_{2\text{ min}}/\text{brain}_{60\text{ min}}$ ratio of [^{18}F]**17** (1.0) was still lower than that of [^{11}C]PIB (12.0)[7,8] or [^{18}F]AV-45 (3.80),[14,15] it was much improved as compared to the values for iodinated benzofuran derivatives

DOI: 10.1021/ml100082x | ACS Med. Chem. Lett. 2010, 1, 321–325

Scheme 3[a]

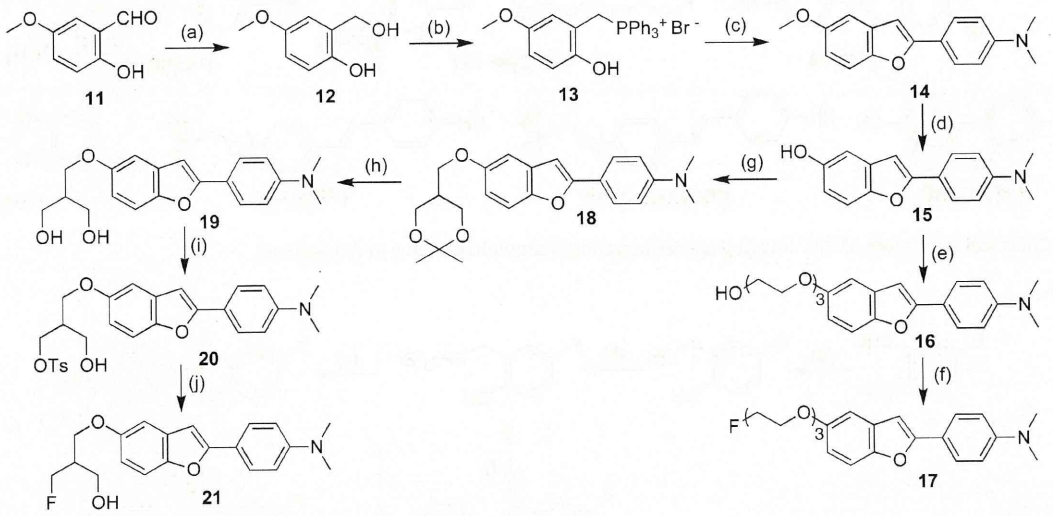

[a] Reagents and conditions: (a) $NaBH_4$, ethanol. (b) Triphenylphosphine hydrobromide, acetonitrile, reflux. (c) 4-Dimethylaminobenzoyl chloride, toluene/NEt_3, reflux. (d) BBr_3/CH_2Cl_2. (e) 2-[2-(2-Chloroethoxy)ethoxy]ethanol, K_2CO_3, DMF, reflux. (f) DAST, DME. (g) 5-(Bromomethyl)-2,2-dimethyl-1,3-dioxane (**10**), K_2CO_3, DMF, 100 °C. (h) HCl, acetone. (i) Tosyl chloride, pyridine, 0 °C. (j) TBAF, THF, reflux.

Scheme 4[a]

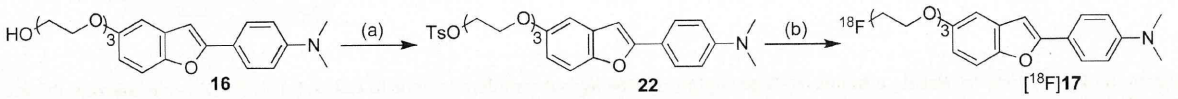

[a] Reagents and conditions: (a) Tosyl chloride, pyridine. (b) Kryptofix222, K_2CO_3, acetonitrile, 120 °C.

Table 1. Chemical Structures and Inhibition Constants of Fluorinated Benzofuran Derivatives

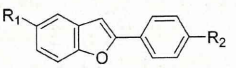

compound	R_1	R_2	K_i (nM)[a]
5	F	NH_2	0.90 ± 0.20
6	F	$NHCH_3$	0.53 ± 0.05
7	F	$N(CH_3)_2$	0.26 ± 0.01
17	$F(CH_2CH_2O)_3$	$N(CH_3)_2$	2.0 ± 0.50
21	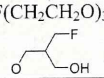	$N(CH_3)_2$	1.0 ± 0.30

[a] Inhibition constants (K_i, nM) of compounds for the binding of [^{125}I]IMPY to Aβ(1−42) aggregates. Values are the means ± standard errors of the mean for 3−6 independent experiments.

(0.47−0.48) reported previously.[17] Furthermore, among these benzofuran derivatives, the washout rate improved as the lipophilicity decreased (log P values of [^{18}F]**17** and the iodinated benzofuran derivatives were 1.20 and 2.12−2.35, respectively).[17] Thus, lipophilicity is important to improving washout from the brain. To further enhance the washout rate, the synthesis of less lipophilic benzofuran derivatives, for example, by replacing the dimethylamino group with another hydrophilic group, is now under investigation. Uptake in the bone at 60 min was measurable (2.74 % ID/g), suggesting little

Table 2. Biodistribution of Radioactivity after Injection of [^{18}F]**17** in Normal Mice[a]

organ	2 min	10 min	30 min	60 min
blood	1.64 ± 0.07	2.48 ± 0.18	2.68 ± 0.26	3.41 ± 0.56
brain	2.88 ± 0.46	5.66 ± 0.31	3.14 ± 0.26	2.80 ± 0.06
bone	1.19 ± 0.18	1.76 ± 0.13	3.63 ± 1.11	2.74 ± 0.59

[a] Expressed as % of injected dose per gram. Each value represents the mean ± SD for five mice.

defluorination in vivo.[13,19,26] However, the free fluoride was not taken up by brain tissue, and so, interference with the imaging is expected to be relatively minor.

Next, to confirm the specific binding of radiofluorinated ligands to β-amyloid plaques, we performed autoradiographic imaging of [^{18}F]**17** with sections (10 μm) of Tg2576 mouse brain. Tg2576 transgenic mice express human APP695 with the K670N, M671L Swedish double mutation.[27] They show marked Aβ deposition in the cingulated cortex, entorhinal cortex, dentate gyrus, and CA1 hippocampal subfield by 11−13 months of age and have been frequently used to evaluate the specific binding of β-amyloid plaques in experiments in vitro and in vivo.[15,18,19,23] Autoradiographic images of [^{18}F]**17** showed high levels of radioactivity in the brain sections (Figure 2A). Furthermore, the hot spots of [^{18}F]**17** corresponded with those of thioflavin-S, a pathological dye commonly used to stain

DOI: 10.1021/ml100082x | ACS Med. Chem. Lett. 2010, 1, 321–325

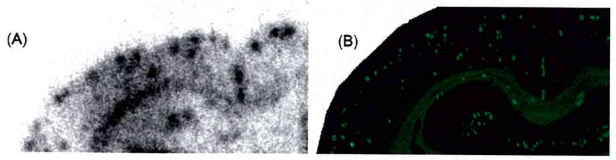

Figure 2. Autoradiography of a section (10 μm) of Tg2576 mouse brain with [^{18}F]**17**. [^{18}F]**17** showed excellent binding to β-amyloid plaques (A). β-Amyloid plaques were confirmed present by staining of the section with thioflavin-S (B).

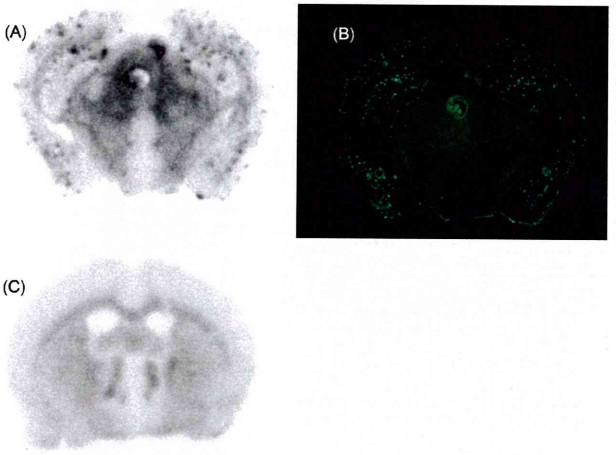

Figure 3. Labeling of β-amyloid plaques in vivo was visualized by autoradiography ex vivo with [^{18}F]**17** in sections of Tg2576 mouse brain (A). The same section was also stained with thioflavin-S (B). Wild-type mouse brain showed no β-amyloid plaques (C).

β-amyloid plaques (Figure 2B). The results suggest that [^{18}F]**17** shows affinity for β-amyloid plaques in the mouse brain in addition to binding synthetic Aβ aggregates.

To further characterize the potential of [^{18}F]**17** as an agent for imaging β-amyloid plaques in living brain tissue, we carried out autoradiography ex vivo in a Tg2576 mouse (36 months, male). The autoradiography showed distinctive labeling of β-amyloid plaques in the brain (Figure 3A), which was confirmed by costaining of the sections with thioflavin-S (Figure 3B). Wild-type mouse brain showed no β-amyloid plaques (Figure 3C). This is consistent with results in vitro showing [^{18}F]**17** to be highly selective in binding to β-amyloid plaques in the brain.

In summary, we produced a series of fluorinated benzofuran derivatives that bind well to Aβ(1−42) aggregates and clearly stain β-amyloid plaques. In experiments in vitro and ex vivo using an animal model of AD, [^{18}F]**17** intensely labeled β-amyloid plaques. These newly synthesized derivatives may become PET radiotracers for imaging β-amyloid plaques in the brain and deserve further investigation by optimizing the substituted groups into the benzofuran backbone.

SUPPORTING INFORMATION AVAILABLE Procedures for the preparation of new fluorinated benzofuran derivatives, in vitro binding assay, in vitro autoradiography using Tg2576 mouse brain sections, and ex vivo autoradiography using Tg2576 mice. This material is available free of charge via the Internet at http://pubs.acs.org.

AUTHOR INFORMATION

Corresponding Author: *To whom correspondence should be addressed. Tel: 81-75-753-4608. Fax: 81-75-753-4568. E-mail: ono@pharm.kyoto-u.ac.jp (M.O.). Tel: 81-75-753-4556. Fax: 81-75-753-4568. E-mail: hsaji@pharm.kyoto-u.ac.jp (H.S.).

Funding Sources: This study was supported by the Program for Promotion of Fundamental Studies in Health Sciences of the National Institute of Biomedical Innovation (NIBIO), a Health Labour Sciences Research Grant, and a Grant-in-Aid for Young Scientists (A) and Exploratory Research from the Ministry of Education, Culture, Sports, Science and Technology, Japan.

REFERENCES

(1) Selkoe, D. J. Alzheimer's Disease: Genes, Proteins, and Therapy. *Physiol. Rev.* **2001,** *81*, 741–766.
(2) Hardy, J.; Selkoe, D. J. The Amyloid Hypothesis of Alzheimer's Disease: Progress and Problems on the Road to Therapeutics. *Science* **2002,** *297*, 353–356.
(3) Selkoe, D. J. Imaging Alzheimer's Amyloid. *Nat. Biotechnol.* **2000,** *18*, 823–824.
(4) Mathis, C. A.; Wang, Y.; Klunk, W. E. Imaging β-Amyloid Plaques and Neurofibrillary Tangles in the Aging Human Brain. *Curr. Pharm. Des.* **2004,** *10*, 1469–1492.
(5) Nordberg, A. PET Imaging of Amyloid in Alzheimer's Disease. *Lancet Neurol.* **2004,** *3*, 519–527.
(6) Ono, M.; Wilson, A.; Nobrega, J.; Westaway, D.; Verhoeff, P.; Zhuang, Z. P. ^{11}C-labeled Stilbene Derivatives as Aβ-Aggregate-Specific PET Imaging Agents for Alzheimer's Disease. *Nucl. Med. Biol.* **2003,** *30*, 565–571.
(7) Mathis, C. A.; Wang, Y.; Holt, D. P.; Huang, G. F.; Debnath, M. L.; Klunk, W. E. Synthesis and Evaluation of ^{11}C-Labeled 6-Substituted 2-Arylbenzothiazoles as Amyloid Imaging Agents. *J. Med. Chem.* **2003,** *46*, 2740–2754.
(8) Klunk, W. E.; Engler, H.; Nordberg, A.; Wang, Y.; Blomqvist, G.; Holt, D. P. Imaging Brain Amyloid in Alzheimer's Disease with Pittsburgh Compound-B. *Ann. Neurol.* **2004,** *55*, 306–319.
(9) Kudo, Y.; Okamura, N.; Furumoto, S.; Tashiro, M.; Furukawa, K.; Maruyama, M.; Itoh, M.; Iwata, R.; Yanai, K.; Arai, H. 2-(2-[2-Dimethylaminothiazol-5-yl]ethenyl)-6-(2-[fluoro]ethoxy)-benzoxazole: A Novel PET Agent for in vivo Detection of Dense Amyloid Plaques in Alzheimer's Disease Patients. *J. Nucl. Med.* **2007,** *48*, 553–561.
(10) Small, G. W.; Kepe, V.; Ercoli, L. M.; Siddarth, P.; Bookheimer, S. Y.; Miller, K. J.; Lavretsky, H.; Burggren, A. C.; Cole, G. M.; Vinters, H. V.; Thompson, P. M.; Huang, S. C.; Satyamurthy, N.; Phelps, M. E.; Barrio, J. R. PET of Brain Amyloid and Tau in Mild Cognitive Impairment. *N. Engl. J. Med.* **2006,** *355*, 2652–2663.
(11) Shoghi-Jadid, K.; Small, G. W.; Agdeppa, E. D.; Kepe, V.; Ercoli, L. M.; Siddarth, P.; Read, S.; Satyamurthy, N.; Petric, A.; Huang, S. C.; Barrio, J. R. Localization of Neurofibrillary Tangles and β-Amyloid Plaques in the Brains of Living Patients with Alzheimer Disease. *Am. J. Geriatr. Psychiatry* **2002,** *10*, 24–35.
(12) Rowe, C. C.; Ackerman, U.; Browne, W.; Mulligan, R.; Pike, K. L.; O'Keefe, G.; Tochon-Danguy, H.; Chan, G.; Berlangieri, S. U.; Jones, G.; Dickinson-Rowe, K. L.; Kung, H. P.; Zhang, W.;

Kung, M. P.; Skovronsky, D.; Dyrks, T.; Holl, G.; Krause, S.; Friebe, M.; Lehman, L.; Lindemann, S.; Dinkelborg, L. M.; Masters, C. L.; Villemagne, V. L. Imaging of Amyloid β in Alzheimer's Disease with ^{18}F-BAY94-9172, A Novel PET Tracer: Proof of Mechanism. *Lancet Neurol.* **2008,** *7*, 129–135.

(13) Zhang, W.; Oya, S.; Kung, M. P.; Hou, C.; Maier, D. L.; Kung, H. F. F-18 Polyethyleneglycol Stilbenes as PET Imaging Agents Targeting Aβ aggregates in the Brain. *Nucl. Med. Biol.* **2005,** *32*, 799–809.

(14) Choi, S. R.; Golding, G.; Zhuang, Z.; Zhang, W.; Lim, N.; Hefti, F.; Benedum, T. E.; Kilbourn, M. R.; Skovronsky, D.; Kung, H. F. Preclinical Properties of ^{18}F-AV-45: A PET Imaging Agent for Aβ Plaques in the Brain. *J. Nucl. Med.* **2009,** *50*, 1887–1894.

(15) Kung, H. F.; Choi, S. R.; Qu, W.; Zhang, W.; Skovronsky, D. ^{18}F Stilbenes and Styrylpyridines for PET Imaging of Aβ Plaques in Alzheimer's Disease. *J. Med. Chem.* **2010,** *53*, 933–941.

(16) Koole, M.; Lewis, D. M.; Buckley, C.; Nelissen, N.; Vandenbulcke, M.; Brooks, D. J.; Vandenberghe, R.; Van Laere, K. Whole-Body Biodistribution and Radiation Dosimetry of ^{18}F-GE067: A Radioligand for in vivo Brain Amyloid Imaging. *J. Nucl. Med.* **2009,** *50* (5), 818–822.

(17) Ono, M.; Kung, M. P.; Hou, C.; Kung, H. F. Benzofuran Derivatives as Aβ Aggregate Specific Imaging Agents for Alzheimer's Disease. *Nucl. Med. Biol.* **2002,** *29*, 633–642.

(18) Ono, M.; Kawashima, H.; Nonaka, A.; Kawai, T.; Haratake, M.; Mori, H.; Kung, M. P.; Kung, H. F.; Saji, H.; Nakayama, M. Novel Benzofuran Derivatives for PET Imaging of β-Amyloid Plaques in Alzheimer's Disease Brains. *J. Med. Chem.* **2006,** *49*, 2725–2730.

(19) Zhang, W.; Oya, S.; Kung, M. P.; Hou, C.; Maier, D. L.; Kung, H. F. F-18 Stilbenes as PET Imaging Agents for Detecting β-Amyloid Plaques in the Brain. *J. Med. Chem.* **2005,** *48*, 5980–5988.

(20) Yuan, W.; Berman, R. J.; Gelb, M. H. Synthesis and Evaluation of Phospholipid Analogues as Inhibitors of Cobra Venom Phospholipase A2. *J. Am. Chem. Soc.* **1987,** *109*, 8071–8081.

(21) Cox, D. P.; Terpinski, J.; Lawrynowicz, W. "Anhydrous" Tetrabutylammonium Fluoride: A Mild but Highly Efficient Source of Nucleophilic Fluoride Ion. *J. Org. Chem.* **1984,** *49*, 3216–3219.

(22) Xu, B.; Stephens, A.; Kirschenheuter, G.; Greslin, A. F.; Cheng, X.; Sennelo, J.; Cattaneo, M.; Zighetti, M. L.; Chen, A.; Kim, S. A.; Kim, H. S.; Bischofberger, N.; Cook, G.; Jacobson, K. A. Acyclic Analogues of Aaenosine Bisphosphates as P2Y Receptor Antagonists: Phosphate Substitution Leads to Multiple Pathways of Inhibition of Platelet Aggregation. *J. Med. Chem.* **2002,** *45*, 5694–5709.

(23) Ono, M.; Watanabe, R.; Kawashima, H.; Cheng, Y.; Kimura, H.; Watanabe, H.; Haratake, M.; Saji, H.; Nakayama, M. Fluoro-Pegylated Chalcones as Positron Emission Tomography Probes for in vivo Imaging of β-amyloid Plaques in Alzheimer's Disease. *J. Med. Chem.* **2009,** *52*, 6394–6401.

(24) Kung, M. P.; Hou, C.; Zhuang, Z. P.; Skovronsky, D.; Kung, H. F. Binding of Two Potential Imaging Agents Targeting Amyloid Plaques in Postmortem Brain Tissues of Patients with Alzheimer's Disease. *Brain Res.* **2004,** *1025*, 98–105.

(25) Kung, M. P.; Hou, C.; Zhuang, Z. P.; Cross, A. J.; Maier, D. L.; Kung, H. F. Characterization of IMPY as a Potential Imaging Agent for β-Amyloid Plaques in Double Transgenic PSAPP Mice. *Eur. J. Nucl. Med. Mol. Imaging* **2004,** *31*, 1136–1145.

(26) Stephenson, K. A.; Chandra, R.; Zhuang, Z. P.; Hou, C.; Oya, S.; Kung, M. P.; Kung, H. F. Fluoro-Pegylated (FPEG) Imaging Agents Targeting Aβ Aggregates. *Bioconjugate Chem.* **2007,** *18*, 238–246.

(27) Hsiao, K.; Chapman, P.; Nilsen, S.; Eckman, C.; Harigaya, Y.; Younkin, S.; Yang, F.; Cole, G. Correlative Memory Deficits, Aβ Elevation, and Amyloid Plaques in Transgenic Mice. *Science* **1996,** *274*, 99–102.

DOI: 10.1021/ml100082x | *ACS Med. Chem. Lett.* **2010,** *1*, 321–325

Bioorganic & Medicinal Chemistry Letters 20 (2010) 5743–5748

Contents lists available at ScienceDirect

Bioorganic & Medicinal Chemistry Letters

journal homepage: www.elsevier.com/locate/bmcl

^{99m}Tc/Re complexes based on flavone and aurone as SPECT probes for imaging cerebral β-amyloid plaques

Masahiro Ono [a,b,*], Ryoichi Ikeoka [a], Hiroyuki Watanabe [a], Hiroyuki Kimura [b], Takeshi Fuchigami [a], Mamoru Haratake [a], Hideo Saji [b], Morio Nakayama [a,*]

[a] Graduate School of Biomedical Sciences, Nagasaki University, 1-14 Bunkyo-machi, Nagasaki 852-8521, Japan
[b] Graduate School of Pharmaceutical Sciences, Kyoto University, 46-29 Yoshida Shimoadachi-cho, Sakyo-ku, Kyoto 606-8501, Japan

ARTICLE INFO

Article history:
Received 30 June 2010
Revised 28 July 2010
Accepted 2 August 2010
Available online 6 August 2010

Keywords:
Alzheimer's disease
β-Amyloid plaque
Single photon emission computed tomography (SPECT)
Imaging

ABSTRACT

Two ^{99m}Tc/Re complexes based on flavone and aurone were tested as potential probes for imaging β-amyloid plaques using single photon emission computed tomography. Both ^{99m}Tc-labeled derivatives showed higher affinity for Aβ(1–42) aggregates than did ^{99m}Tc-BAT. In sections of brain tissue from an animal model of AD, the Re-flavone derivative **9** and Re-aurone derivative **19** intensely stained β-amyloid plaques. In biodistribution experiments using normal mice, ^{99m}Tc-labeled flavone and aurone displayed similar radioactivity pharmacokinetics. With additional modifications to improve their brain uptake, ^{99m}Tc complexes based on the flavone or aurone scaffold may serve as probes for imaging cerebral β-amyloid plaques.

Alzheimer's disease (AD) is a neurodegenerative disorder of the brain associated with irreversible cognititive decline, memory impairment, and behavioral changes. Currently, the only definitive confirmation of AD is by postmortem histopathological examination of β-amyloid plaques in the brain. The early appraisal of clinical symptoms for a diagnosis of AD is often difficult and unreliable. Numerous reports suggest the accelerated accumulation of β-amyloid plaques in the brain to be a key risk factor associated with AD. Consequently, the detection of individual β-amyloid plaques in vivo by single photon emission computed tomography (SPECT) or positron emission tomography (PET) should improve the diagnosis of and also accelerate the discovery of effective therapeutic agents for AD.[1–4] Many PET/SPECT probes for imaging β-amyloid based on Congo Red, thioflavin T, and DDNP have been reported. Among them, [^{11}C]PIB,[5,6] [^{11}C]SB-13,[7,8] [^{18}F]BAY94-9172,[9,10] [^{11}C]BF-227,[11] [^{18}F]FDDNP,[12,13] [^{123}I]IMPY,[14–16] and [^{18}F]AV-45[17,18] have been tested clinically and demonstrated potential utility. There are more SPECT scanners than PET imaging devices installed for routine clinical imaging, which provides a certain advantage to using SPECT imaging agents. Since SPECT is more valuable than PET in terms of routine diagnostic use, the development of more useful Aβ imaging agents for SPECT has been a critical issue. Although many radioiodinated SPECT imaging agents for detecting β-amyloid plaques have been reported, there are few reports on the development of ^{99m}Tc imaging agents.

^{99m}Tc ($T_{1/2}$ = 6.01 h, 141 keV) has become the most commonly used radionuclide in diagnostic nuclear medicine by SPECT for several reasons: it is readily produced by an ^{99}Mo/^{99m}Tc generator, the gamma-ray energy it emits is suitable for detection, and its physical half-life is compatible with the biological localization and residence time required for imaging. Its ready availability, essentially 24 h a day, and easiness of use make it the radionuclide of choice. New ^{99m}Tc-labeled imaging agents will provide simple, convenient, and widespread SPECT-based imaging methods for detecting and eventually quantifying β-amyloid plaques in living brain tissue.

It has been reported that a dopamine transporter imaging agent, [^{99m}Tc]TRODAT-1, is useful to detect the loss of dopamine neurons in the basal ganglia associated with Parkinson's disease. This is the first example of a ^{99m}Tc imaging agent that can penetrate the blood–brain barrier via a simple diffusion mechanism and localize at sites in the central nervous system. Based on this success, efforts were made to search for comparable ^{99m}Tc imaging agents that target binding sites on β-amyloid plaques in the brain of AD patients. Several ^{99m}Tc-labeled imaging probes have been developed (Fig. 1), but no clinical study of them has been reported.[19–22]

Recently, we have reported that flavonoids including chalcone, flavone, and aurone serve as useful molecular scaffolds in the development of imaging agents for β-amyloid plaques in the brain.[23–28] Initially, we designed and synthesized four ^{99m}Tc-labeled chalcone derivatives with monoamine-monoamide

* Corresponding authors.
E-mail address: ono@pharm.kyoto-u.ac.jp (M. Ono).

0960-894X/$ - see front matter © 2010 Elsevier Ltd. All rights reserved.
doi:10.1016/j.bmcl.2010.08.004

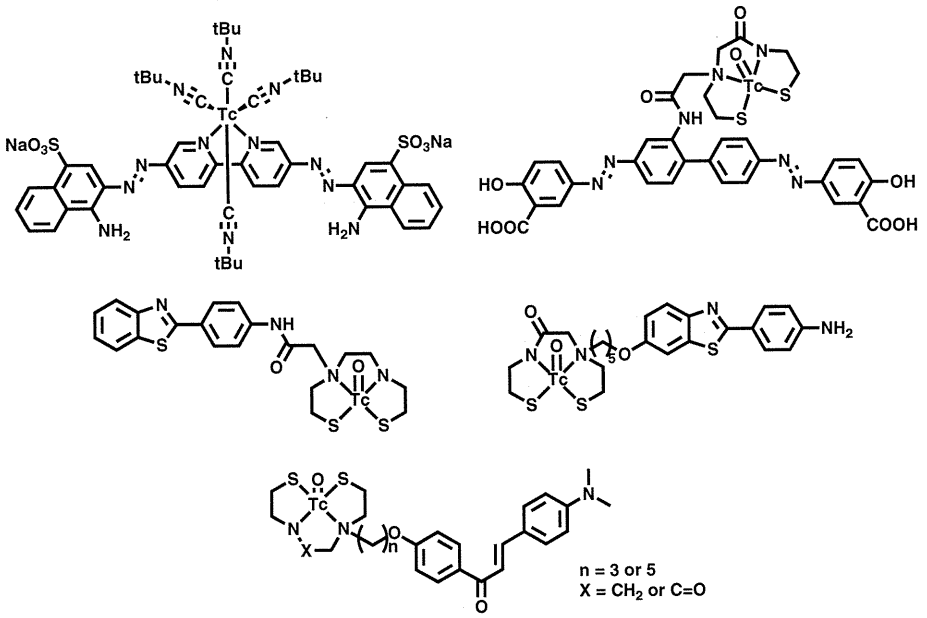

Figure 1. Chemical structure of ^{99m}Tc-labeled Aβ imaging probes reported previously.

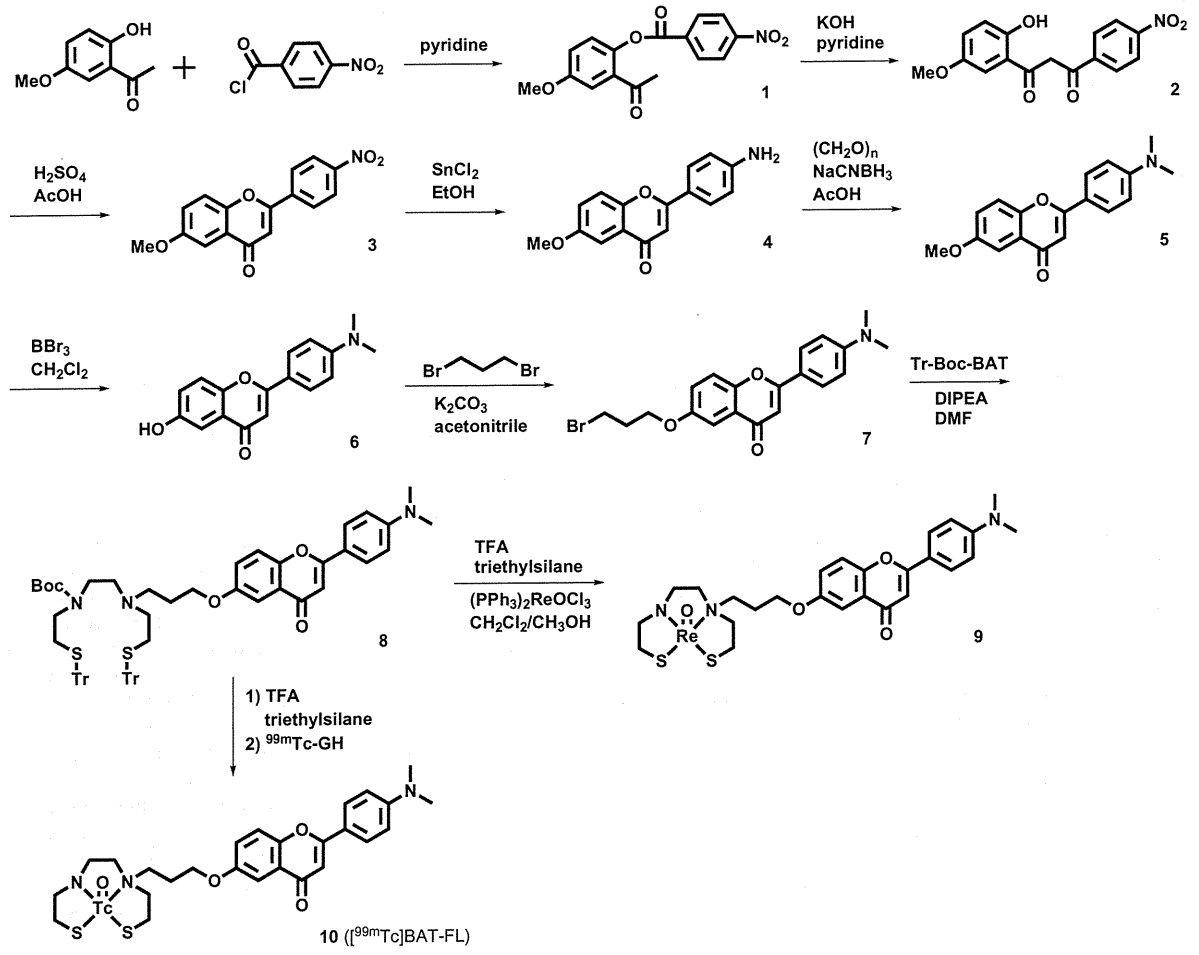

Scheme 1. Synthesis of flavone derivatives.

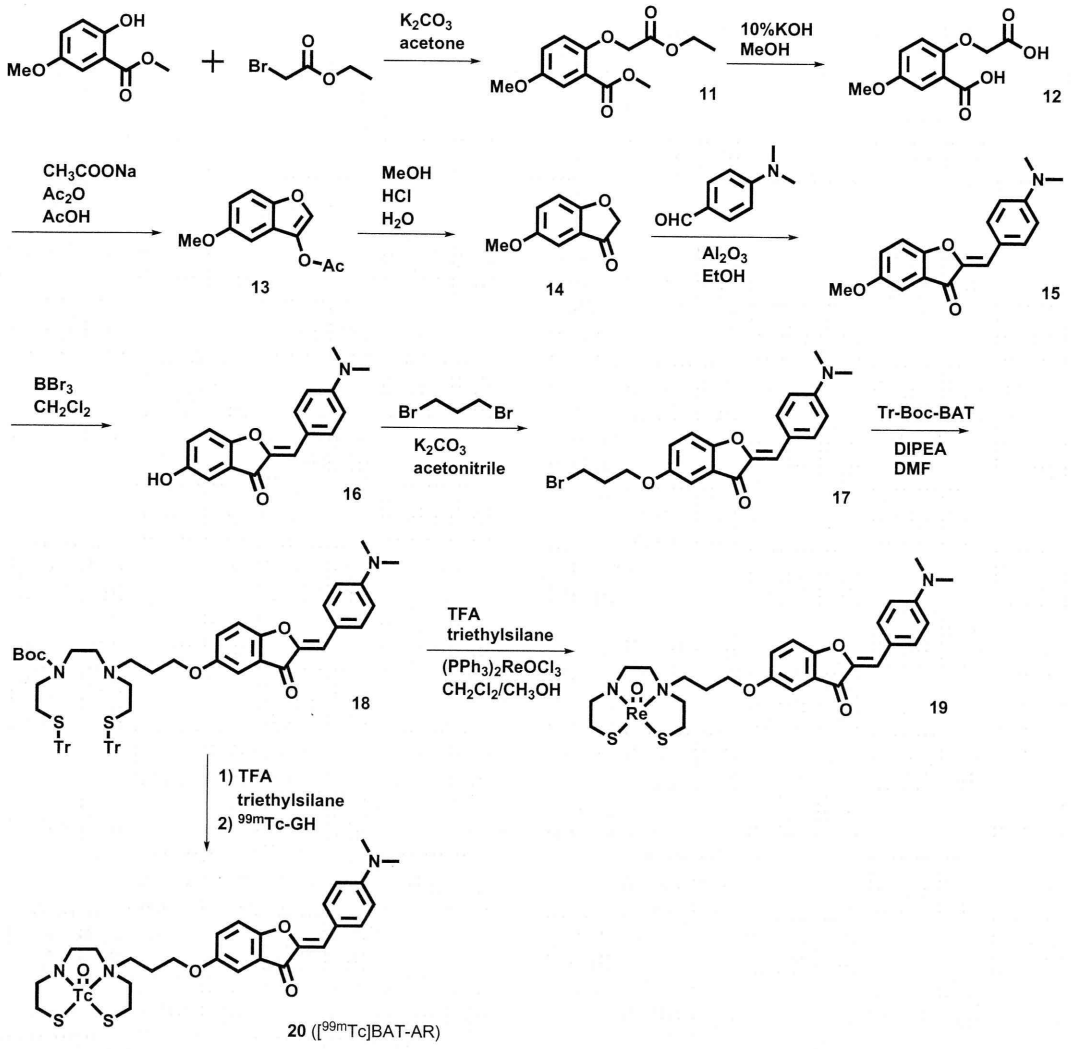

Scheme 2. Synthesis of aurone derivatives.

dithiol (MAMA) and bis-amino-bis-thiol (BAT) (Fig. 1).[29] MAMA and BAT were selected as a chelation ligand taking into consideration the permeability of the blood–brain barrier, because they form an electrically neutral complex with ^{99m}Tc.[30] ^{99m}Tc-BAT-chalcone ($n = 3$) (Fig. 1) showed good uptake into and rapid clearance from the brain in addition to high affinity for β-amyloid plaques, indicating it may be a promising probe for the detection of β-amyloid plaques in the brain.[29] Based on the positive results, we decided to further develop new ^{99m}Tc imaging agents based on the flavonoid scaffold.

In the present study, to develop more useful ^{99m}Tc imaging agents for the clinical diagnosis of AD, we synthesized two flavone and aurone derivatives with BAT as a chelation ligand. We then evaluated the biological potential of these compounds as probes by testing their affinity for Aβ aggregates and β-amyloid plaques in sections of brain tissue from Tg2576 mice and their uptake by and clearance from the brain in biodistribution experiments using normal mice. Also, we compared their usefulness as Aβ imaging probes with a ^{99m}Tc-labeled chalcone derivative reported previously.[29] To our knowledge, this is the first time ^{99m}Tc/Re complexes based on flavone and aurone scaffolds have been proposed as probes for the detection of β-amyloid plaques in the brain.

The synthesis of the ^{99m}Tc/Re complexes based on flavone and aurone was outlined in Schemes 1 and 2. The chelation ligand (BAT) was synthesized according to methods reported previously with some slight modifications.[30] The most useful method of preparing flavones is known as the Baker–Venkataraman transformation.[23] A hydroxyacetophenone was first converted into a benzoyl ester (**1**) which was then treated with a base, forming a 1,3-diketone (**2**). Treatment of this diketone with acid led to the generation of the desired flavone (**3**). The free amino derivative **4** was readily prepared from **3** by reduction with $SnCl_2$ (92% yield). Conversion of **4** to the dimethylamino derivative **5** was achieved by a method reported previously (83% yield). Compound **5** was converted to **6** by demethylation with BBr_3 in CH_2Cl_2 (40% yield). The reaction of dibromopentane with **6** produced the flavone derivative **7** with a trimethine group. Then, **7** was joined to Tr-Boc-BAT to generate **8** (the precursor of ^{99m}Tc/Re reaction). The target aurone derivatives were prepared as shown in Scheme 2. The synthesis of the aurone backbone was achieved via an Aldol reaction of benzofuranones with benzaldehydes using Al_2O_3. 5-Methozy-3-benzofuranone (**14**) was reacted with 4-dimethybenzaldehyde in the presence of Al_2O_3 in chloroform at room temperature to form **15** in a yield of 92%. The precursor of the reaction with ^{99m}Tc/Re, **18**, was obtained

Table 1
HPLC retention times of ^{99m}Tc/Re compounds and log *P* of ^{99m}Tc compounds

Re compounds	Retention time[a] (min)	^{99m}Tc compounds	Retention time[a] (min)	Log *P* of ^{99m}Tc compounds[b]
9	9.5	**10**	11.1	2.77 ± 0.04
19	14.6	**20**	16.6	2.23 ± 0.04

[a] Reversed-phase HPLC using a mixture of H_2O–acetonitrile (2:3) as a mobile phase.
[b] The measurement was done in triplicate and repeated three times. Each value represents the mean ± SD for three independent experiments.

as described for the synthesis of the flavone derivative **8**. After deprotection of the thiol groups in **8** and **18** in TFA and triethylsilane, the Re complexes (**9** and **19**) were prepared through a reaction with $(PPh_3)_2ReOCl_3$. The corresponding ^{99m}Tc complexes, **10** ([^{99m}Tc]BAT-FL) and **20** ([^{99m}Tc]BAT-AR), were prepared by a ligand exchange reaction employing the precursor ^{99m}Tc-glucoheptonate (GH). The resulting mixture was analyzed by reversed-phase HPLC, showing that a single radioactive complex formed with radiochemical purity higher than 95% after purification by HPLC. The identity of the complex was established by comparative HPLC using the corresponding Re complexes as a reference (Table 1). The retention times for [^{99m}Tc]BAT-FL and [^{99m}Tc]BAT-AR on HPLC (radioactivity) were 11.1 and 16.6 min, respectively. The retention times of the corresponding Re complexes on HPLC (UV detection) were 9.5 and 14.6 min, respectively.

In vitro binding experiments to evaluate the affinity of [^{99m}Tc]BAT-FL and [^{99m}Tc]BAT-AR for Aβ(1–42) aggregates were carried out in solutions. The percent radioactivity of [^{99m}Tc]BAT-FL and [^{99m}Tc]BAT-AR bound to aggregates increased dependent on the dose of Aβ(1–42), while [^{99m}Tc]BAT showed no marked affinity for the aggregates (Fig. 2). At all concentrations of Aβ aggregates, [^{99m}Tc]BAT-AR showed significantly greater affinity than [^{99m}Tc]BAT-FL. In these binding experiments, the non-specific binding of [^{99m}Tc]BAT-FL and [^{99m}Tc]BAT-AR was estimated at 1.62–1.85%. The affinity of [^{99m}Tc]BAT-FL and [^{99m}Tc]BAT-AR was less than that of ^{99m}Tc-labeled chalcone derivatives reported previously (Fig. 1).[29] The order in terms of strength of binding corresponded with that of radioiodinated flavonoids,[23–25] indicating that the scaffolds of the [^{99m}Tc]BAT complexes did not play an important role in the affinity for Aβ aggregates.

To confirm the affinity for β-amyloid plaques in the mouse brain, neuropathological fluorescent staining with Re derivatives (**9** and **19**) was carried out using Tg2576 mouse brain sections (Fig. 3). Many β-amyloid plaques were clearly stained with the derivatives (Fig. 3A and B), as reflected by the high affinity for Aβ aggregates in binding assays in vitro. The labeling pattern was consistent with that observed with thioflavin S (Fig.3C and D). These results suggest that [^{99m}Tc]BAT-FL and [^{99m}Tc]BAT-AR would bind to β-amyloid plaques in the mouse brain in addition to having affinity for synthetic Aβ(1–42) aggregates. Although [^{99m}Tc]BAT-AR showed greater affinity than [^{99m}Tc]BAT-AR in the binding assays in vitro, no marked difference in binding between [^{99m}Tc]BAT-FL and [^{99m}Tc]BAT-AR was observed in the fluorescent staining experiments.

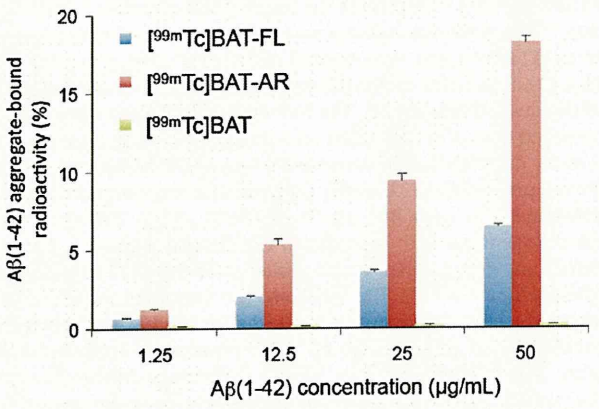

Figure 2. Binding assay of [^{99m}Tc]BAT-FL, [^{99m}Tc]BAT-AR, and [^{99m}Tc]BAT with Aβ(1–42) aggregates. Values are the mean ± standard error of the mean for three independent experiments.

[^{99m}Tc]BAT-FL and [^{99m}Tc]BAT-AR were examined as to their biodistribution in normal mice (Table 2). A biodistribution study provides important information on brain uptake. The ideal probe for imaging β-amyloid should penetrate the blood–brain barrier well enough to deliver a sufficient dose into the brain while clearing rapidly from normal regions so as to achieve a high signal to noise ratio in the AD brain. Previous studies suggest that the optimal lipophilicity for entry into the brain is obtained with log *P* values of between 1 and 3. [^{99m}Tc]BAT-FL and [^{99m}Tc]BAT-AR had log *P* values of 2.77 and 2.23, respectively (Table 1), but showed less uptake, 0.64 and 0.79%ID/g at 2 min postinjection, than expected. Thereafter, the radioactivity of [^{99m}Tc]BAT-FL and [^{99m}Tc]BAT-AR that accumulated in the brain was rapidly eliminated (0.23 and 0.11%ID/g at 60 min postinjection). Recently, we have reported that the ^{99m}Tc-labeled chalcone derivative showed high uptake (1.48%ID/g at 2 min postinjection) into and rapid clearance (0.17%ID/g at 60 min postinjection) from the brain, a highly desirable property for imaging agents for β-amyloid plaques.[29] The pharmacokinetics of the ^{99m}Tc-labeled chalcone derivative in the brain appears superior to that of any ^{99m}Tc-labeled probes reported previously, indicating that this compound should be investigated further as a potentially useful probe for imaging β-amyloid. Compared with that of the ^{99m}Tc-labeled chalcone,[29] the radioactivity of [^{99m}Tc]BAT-FL and [^{99m}Tc]BAT-AR appears insufficient for the imaging of β-amyloid plaques in the brain. Since the affinity of [^{99m}Tc]BAT-FL and [^{99m}Tc]BAT-AR for Aβ aggregates was as high as that of ^{99m}Tc-labeled chalcone derivatives,[29] improvement of the uptake of [^{99m}Tc]BAT-FL and [^{99m}Tc]BAT-AR is an important prerequisite to developing more useful ^{99m}Tc-labeled probes. Therefore, additional structural changes in the flavone and aurone scaffold are needed to further improve the pharmacokinetics of [^{99m}Tc]BAT-FL and [^{99m}Tc]BAT-AR in vivo.

In conclusion, we successfully designed and synthesized novel ^{99m}Tc/Re complexes based on flavone and aurone for the detection of β-amyloid plaques in the brain. Both [^{99m}Tc]BAT-FL and [^{99m}Tc]BAT-AR showed high affinity for synthetic Aβ(1–42) aggregates. In experiments in vitro using sections of brain from Tg2576 mice, Re complexes intensely stained β-amyloid plaques. In addition, [^{99m}Tc]BAT-FL and [^{99m}Tc]BAT-AR displayed good uptake into and a rapid washout from the brain after their injection in normal mice. This combination of affinity for β-amyloid plaques, and good uptake and clearance makes [^{99m}Tc]BAT-FL and [^{99m}Tc]BAT-AR promising probes for the detection of β-amyloid plaques in the brain, although additional modifications are required to enhance their uptake. The results of the present study should provide information useful for the development of ^{99m}Tc-labeled probes for the imaging of β-amyloid plaques in the brain.